

Electronic Supplementary Information

Unsymmetrical Starburst Triarylamines: Synthesis, Properties, and Characteristics of OFETs

Dheepika Ramachandran,^a Srinitha Sonalin,^a Predhanekar Mohamed Imran,^b Samuthira Nagarajan^{*a}

^a*Department of Chemistry, Central University of Tamil Nadu, Thiruvarur- 610 005, India.*

**Email: snagarajan@cutn.ac.in*

^b*Department of Chemistry, Islamiah College, Vaniyambadi - 635 752, India.*

Table of Contents

| | |
|---|----------|
| Materials and instruments..... | S2 |
| General considerations..... | S2 |
| Experimental procedures and analytical data..... | S2 |
| Figure S1. DSC thermogram of compounds 1-8 | S6 |
| Table S1. Thermal behavior of compounds 1-8 | S6 |
| Figure S2. OFET device schematic representation..... | S7 |
| Figure S3. Non-contact mode AFM and SEM images of thin films..... | S7 |
| Figure S4. Generalized representation of molecule | S8 |
| Table S2. Geometrical parameters of predicted single crystals 1-8 at ground state S₀ | S8 |
| Table S3. Crystal structure and lattice parameters at ground level S₀ | S9 |
| Table S4. Interatomic distance, band gap and mobility of compounds 1-8 | S9 |
| Figure S5. Spatial distributions of FMOs of compounds 1-8 | S9 |
| Figure S6. Density of States graphs of compounds 1-8 | S10, S11 |
| Figure S7. Polymorph predictions at polycrystalline level | S12, S13 |
| Figure S8. Hopping distance prediction in poly crystalline packing | S13, S14 |
| Figure S9. ¹ H NMR and ¹³ C NMR spectra of compound 2 | S15 |
| Figure S10. HR-Mass spectra of compound 2 | S16 |
| Figure S11. ¹ H NMR and ¹³ C NMR spectra of compound 3 | S17 |
| Figure S12. HR-Mass spectra of compound 3 | S18 |
| Figure S13. ¹ H NMR and ¹³ C NMR spectra of compound 4 | S19 |
| Figure S14. HR-Mass spectra of compound 4 | S20 |
| Figure S15. ¹ H NMR and ¹³ C NMR spectra of compound 5 | S21 |
| Figure S16. HR-Mass spectra of compound 5 | S22 |
| Figure S17. ¹ H NMR and ¹³ C NMR spectra of compound 6 | S23 |
| Figure S18. HR-Mass spectra of compound 6 | S24 |
| Figure S19. ¹ H NMR and ¹³ C NMR spectra of compound 7 | S25 |
| Figure S20. HR-Mass spectra of compound 7 | S26 |
| Figure S21. ¹ H NMR and ¹³ C NMR spectra of compound 8 | S27 |
| Figure S22. HR-Mass spectra of compound 8 | S28 |

Materials and instruments

Triphenylamine, POCl₃, tetrakis (triphenylphosphine) palladium, and all the boronic acids (naphthyl boronic acid, biphenyl boronic acid, thiophene-3-boronic acid, benzenboronic acid, 4- methoxy phenyl boronic acid, 3-nitrophenyl boronic acid, 4-trifluoromethyl boronic acid) were used as purchased from the commercial sources. N, N-Dimethylformamide (DMF) and triethylamine used were anhydrous. All the other solvents (AR grade) were used as received.

¹H NMR and ¹³C NMR were recorded in Bruker 400 MHz spectrometer in CDCl₃. Chemical shifts reported against TMS. Absorption spectra of compounds were measured by JASCO UV-NIR spectrophotometer. Fluorescence measurements were obtained from Perkin Elmer Spectrofluorimeter LS55. Electrochemical studies were done with CH Instruments: Electrochemical Workstation (CHI 6035D). Perkin Elmer FT-IR was employed to read about the characteristic functional groups. High-resolution mass spectra were recorded in ThermoExactPlus UHPLC-MS. Thermal studies carried out in TA thermal analyser.

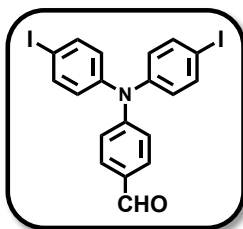
General considerations

All the photophysical properties were investigated at room temperature in anhydrous dichloromethane solvent, concentration was fixed 10⁻⁵M for absorption spectra and 10⁻⁷M for emission spectra. Electrochemical behaviour of the synthesised compounds were investigated using CHI-Electrochemical Workstation at room temperature. Electrochemical cell was comprised of glassy carbon working electrode, Pt wire as counter electrode and a SCE (saturated calomel electrode) reference electrode. The system was calibrated externally using Fc/Fc⁺ as a standard. Working electrode was polished thoroughly with Alumina (1, 0.5 and 0.3 micron respectively) and used. 0.1M solution of tetrabutylammonium hexafluorophosphate in CH₃CN was the supporting electrolyte. Thermal behaviour was investigated in N₂ atmosphere at a scan rate of 10°C per minute.

Experimental procedure

Compound **1** was synthesized from a two-step synthetic sequence of Vilsmyer-Hack formylation followed by iodination of commercially available triphenylamine (TPA) **Scheme 1**. Then the precursor was subjected Pd-catalysed Suzuki coupling reactions to reach the desired products. All the molecules were confirmed spectroscopically and characterized.

4-(Bis(4-iodophenyl)amino)benzaldehyde **1**:

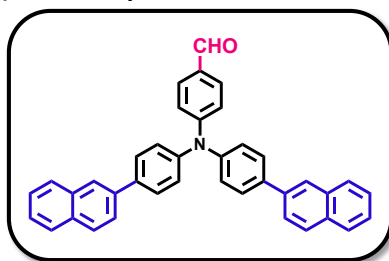


(a) Vilsmyer-Hack formylation: Phosphorus oxychloride (1.85 mL, 20 mmol) was added dropwise to DMF (5.6 mL, 73 mmol) which was stirred at 0°C and this formylating mixture was allowed to stir for an hour in same condition. To this triphenylamine (5 g, 20 mmol) was added, temperature raised to 80 °C and continued for 4 hours. As monitored by TLC, reaction mixture was cooled to room temperature and quenched with water. Neutralised by 20 % aqueous NaOH. Brownish yellow product was washed with water and extracted with DCM finally washed with brine solution and dried over anhydrous Na₂SO₄. Purified by column chromatography using 2% ethyl acetate in hexane. Pale yellow solid (4.8 g, 88 %) (b) Iodination: Under stirring 4-(diphenylamino)benzaldehyde (2.5 g, 9.2 mmol) was dissolved in 10 mL of glacial acetic acid and 2 mL water with KI (2 g, 11.9 mmol) and allowed to stir at 80 °C for one hour. Then KIO₃ (1.91 g, 9.2 mmol) was added and reaction continued for 3 hours at 100°C. Monitored by TLC. After completion of reaction

quenched with water and cooled to room temperature. Formed brown yellow precipitate (4.45 g, 92 %) was filtered under pressure washed with plenty of water to remove excess of acetic acid.

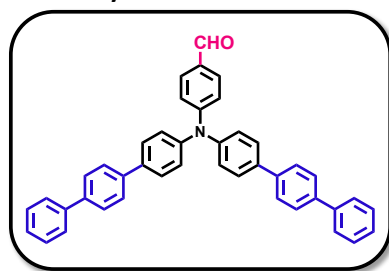
General procedure for Suzuki coupling: 4-(Bis(4-iodophenyl)amino)benzaldehyde **1** (500 mg, 0.95 mmol) is dissolved in anhydrous THF and 2 M aqueous Na_2CO_3 . 10 mol% of $\text{Pd}(\text{PPh}_3)_4$ added under N_2 atmosphere at room temperature and stirred for 20 minutes then corresponding boronic acid added and temperature raised to reflux. Reaction continued for 7 hours and monitored by TLC. After that cooled to room temperature and solvent removed under vacuum. Remaining residue extracted with DCM washed thrice with distilled water finally with brine solution dried over anhydrous Na_2SO_4 . Purified by column chromatography (SiO_2) in hexane ethyl acetate system.

4-(Bis(4-(naphthalen-2-yl)phenyl)amino)benzaldehyde 2:



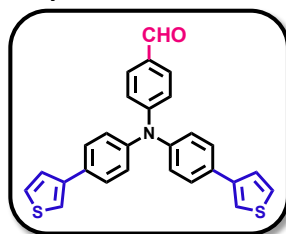
Yellow solid. Yield: 80%. ^1H NMR (400MHz, CDCl_3): δ (ppm) 9.86 (s, 1H), 8.05 (s, 2H), 7.94-7.86 (m, 6H), 7.76-7.71 (m, 8H), 7.53-7.47 (m, 4H), 7.33 (d, $J = 8.4\text{Hz}$, 4H), 7.19 (d, $J = 8.4\text{Hz}$, 2H) ^{13}C NMR (100 MHz, CDCl_3): δ (ppm) 190.57, 153.12, 145.49, 137.73, 137.55, 133.72, 132.65, 131.46, 129.60, 128.67, 128.51, 128.23, 127.73, 126.48, 126.45, 126.34, 126.09, 125.55, 125.27, 120.21. HRMS (ESI) m/z calcd for $\text{C}_{39}\text{H}_{27}\text{NO}$ [$\text{M}+\text{H}$] 526.2171, found 526.2178.

4-(Di([1,1':4',1''-terphenyl]-4-yl)amino)benzaldehyde 3:



Yellow solid. Yield: 69%. ^1H NMR (400MHz, CDCl_3): δ (ppm) 9.85 (s, 1H), 7.74 (d, $J = 8.4\text{Hz}$, 2H), 7.69 (s, 8H), 7.66-7.63 (t, 8H), 7.48-7.45 (t, $J = 7.2\text{Hz}$, 2H), 7.38-7.35 (t, $J = 7.2\text{Hz}$, 2H), 7.29(d, $J = 8.4\text{Hz}$, 2H), 7.17(d, $J = 8\text{Hz}$, 2H). ^{13}C NMR (100 MHz, CDCl_3): δ (ppm) 190.49, 153.08, 145.44, 140.59, 140.17, 139.11, 137.31, 131.40, 129.61, 128.87, 128.25, 127.59, 127.43, 127.22, 127.03, 126.37, 120.19, HRMS (ESI) m/z calcd for $\text{C}_{43}\text{H}_{31}\text{NO}$ [$\text{M}+\text{H}$] 577.2406, found 577.2486.

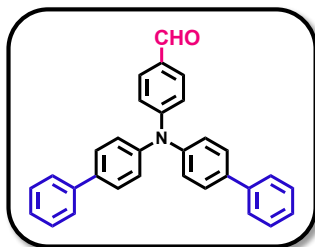
4-(Bis(4-(thiophen-3-yl)phenyl)amino)benzaldehyde 4:



Yellow solid. Yield: 92%. ^1H NMR (400MHz, CDCl_3): δ (ppm) 9.87 (s, 1H), 7.70 (d, $J=8.8\text{Hz}$, 2H), 7.57 (d, $J=8.4\text{Hz}$, 2H), 7.42 (s, 1H), 7.42-7.33 (m, 4H), 7.20-7.17(m, 5H), 7.07 (d, $J=8.8\text{Hz}$, 2H) ^{13}C NMR (100 MHz, CDCl_3): δ (ppm) 153.20, 146.06,

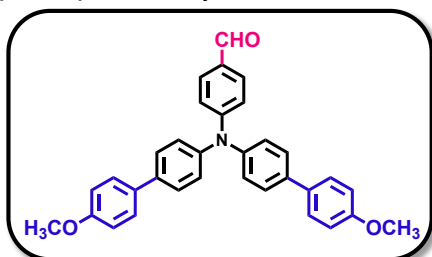
145.12, 141.47, 132.60, 131.36, 129.81, 129.75, 129.29, 127.65, 126.44, 126.35, 126.34, 126.13, 125.23, 125.14, 120.14, 119.65, 119.36. HRMS (ESI) m/z calcd for $C_{27}H_{19}NO_2$ [M+H] 437.090, found 437.0863.

4-(Di([1,1'-biphenyl]-4-yl)amino)benzaldehyde 5:



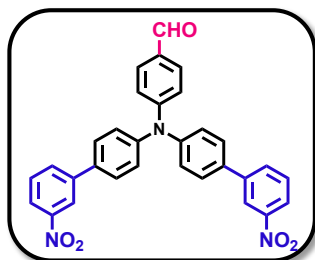
Half white solid. Yield: 86.4%. 1H NMR (400MHz, $CDCl_3$) δ (ppm): 9.84 (s, 1H), 7.74 (d, 2H), 7.60 (dd, 8H), 7.47 (t, 4H), 7.37 (t, 2H), 7.26 (d, 4H), 7.15 (d, $J=8.8$ Hz, 2H) ^{13}C NMR (100 MHz, $CDCl_3$): δ (ppm) 190.52, 153.12, 145.35, 140.24, 137.87, 131.40, 129.49, 128.88, 128.37, 127.35, 126.89, 126.35, 120.04. HRMS (ESI) m/z calcd for $C_{31}H_{23}NO$ [M+H] 426.1858, found 426.1852.

4-(Bis(4'-methoxy-[1,1'-biphenyl]-4-yl)amino)benzaldehyde 6:



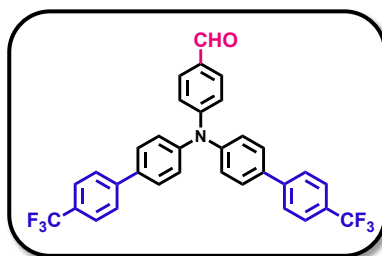
White solid. Yield: 91%. 1H NMR (400MHz, $CDCl_3$): δ (ppm) 9.82 (s, 1H), 7.72 (d, $J=8.8$ Hz, 2H), 7.54 (dd, 8H), 7.25 (d, $J=8.4$ Hz, 4H), 7.13 (d, $J=8.8$ Hz, 2H), 6.99 (d, $J=8.8$ Hz, 4H), 3.86 (s, 3H) ^{13}C NMR (100 MHz, $CDCl_3$): δ (ppm) 190.48, 159.19, 153.23, 144.74, 137.57, 132.78, 131.38, 129.22, 127.91, 127.87, 126.44, 119.63, 114.30, 55.37. HRMS (ESI) m/z calcd for $C_{33}H_{27}NO_3$ [M+H] 486.2069, found 486.2072.

4-(Bis(3'-nitro-[1,1'-biphenyl]-4-yl)amino)benzaldehyde 7:



Brown solid. Yield: 85.2%. 1H NMR (400MHz, $CDCl_3$): δ (ppm) 9.88 (s, 1H), 8.46 (t, 2H), 8.22 (dd, 2H), 7.93 (d, $J=7.6$ Hz, 2H), 7.79 (d, $J=8.8$ Hz, 2H), 7.65-7.61 (m, 7H), 7.32 (d, $J=8.4$ Hz, 4H), 7.21 (d, $J=8.8$ Hz, 2H) ^{13}C NMR (100 MHz, $CDCl_3$): δ (ppm) 190.53, 152.54, 148.80, 146.51, 141.87, 135.11, 132.69, 131.45, 130.40, 129.88, 128.56, 126.26, 123.27, 122.08, 121.67, 121.18. HRMS (ESI) m/z calcd for $C_{31}H_{21}N_3O_5$ [M+H] 516.1554, found 516.1504.

4-(Bis(4'-(trifluoromethyl)-[1,1'-biphenyl]-4-yl)amino)benzaldehyde 8:



Brown solid. Yield: 92.7%. ^1H NMR (400MHz, CDCl_3): δ (ppm) 9.87 (s, 1H), 7.83 (t, 2H), 7.78-7.74 (m, 4H), 7.69-7.68 (m, 1H), 7.62-7.55 (m, 8H), 7.38 (d, 1H), 7.30 (d, $J=8.8\text{Hz}$, 4H), 7.18(d, $J=8.4\text{Hz}$, 2H) ^{13}C NMR (100 MHz, CDCl_3): δ (ppm) 190.50, 152.77, 146.06, 141.02, 136.30, 135.23, 131.77, 131.45, 131.41, 131.13, 130.81, 130.25, 130.11, 130.05, 129.37, 128.52, 128.22, 127.72, 127.67, 127.61, 126.31, 125.51, 124.02, 123.98, 123.73, 123.69, 123.65, 123.61, 122.80, 120.69, 120.10. HRMS (ESI) m/z calcd for $\text{C}_{33}\text{H}_{21}\text{NOF}_6$ $[\text{M}+\text{H}]$ 562.160, found 562.157.

Thermal behaviour of molecules

Thermal stability and morphology of the molecules play an important role in electronics, especially to improve lifetime and efficiency of the device. **Figure 4** shows the DSC behavior of compounds at a heating rate of $10\text{ }^\circ\text{C min}^{-1}$ under nitrogen atmosphere. Melting points were observed as sharp peaks and decomposition was observed as broad curves around $400\text{ }^\circ\text{C}$. Compound **3** has the high melting point $243\text{ }^\circ\text{C}$ and heat capacity calculated was 89.6 J/g . Comparing all molecules with **1**, it is evident that their melting temperature increased greatly, concluding that thermal stability of all the new π extended molecules is upgraded and durability of the devices assured. Values extracted from differential calorimetric analysis are given in **Table 3**. Interestingly, compounds **4** and **5** are showing two sharp melting peaks and the reason may be the existence of polymorphs. Compounds are showing comparatively high decomposition temperature ($\sim 400\text{ }^\circ\text{C}$) than other triarylamine compounds¹¹.

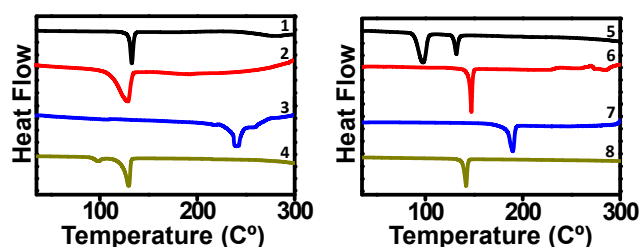


Figure S1. DSC thermogram of compounds 1-8

Table 1. Thermal behavior of compounds 1-8

| | T_m $^\circ\text{C}$ | T_d $^\circ\text{C}$ | Heat capacity J/g |
|----------|------------------------|------------------------|----------------------|
| 1 | 130 | 247 | 92.9 |
| 2 | 124 | 469 | 85.2 |
| 3 | 243 | 412 | 89.6 |
| 4 | 92, 130 | 425 | 2.4, 20.7 |
| 5 | 93, 128 | 398 | 11.8, 2 |
| 6 | 191 | 389 | 167.9 |
| 7 | 182 | 418 | 70.4 |
| 8 | 137 | 427 | 52.3 |

Schematic representation of fabricated device

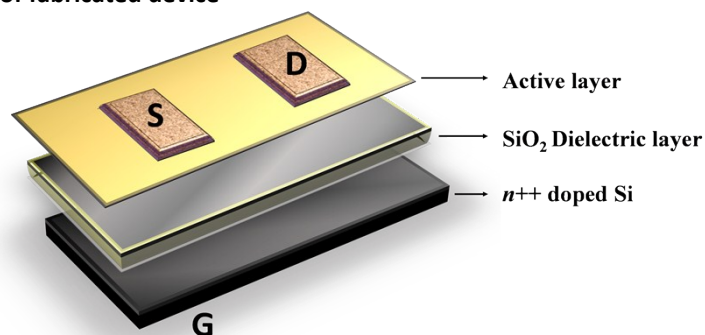


Figure S2. Schematic representation of OFET device

FET architecture opted for device fabrication was bottom gate top contact as represented in the **Figure S1**. Active semiconducting material coated over SiO₂ and annealed at 60 °C to remove the residual solvents.

Film morphology

To have a clear vision about the device performance, morphology of the active layer was investigated. Films over SiO₂ dielectric layer was analysed by non-contact mode atomic force microscopy (AFM) and scanning electron microscope (SEM). 2 and 3 dimensional images of films obtained by AFM are given in the **Figure S2**. The surface roughness was 0.987 nm for compound **2**, 1nm for compound **3** and **4**.

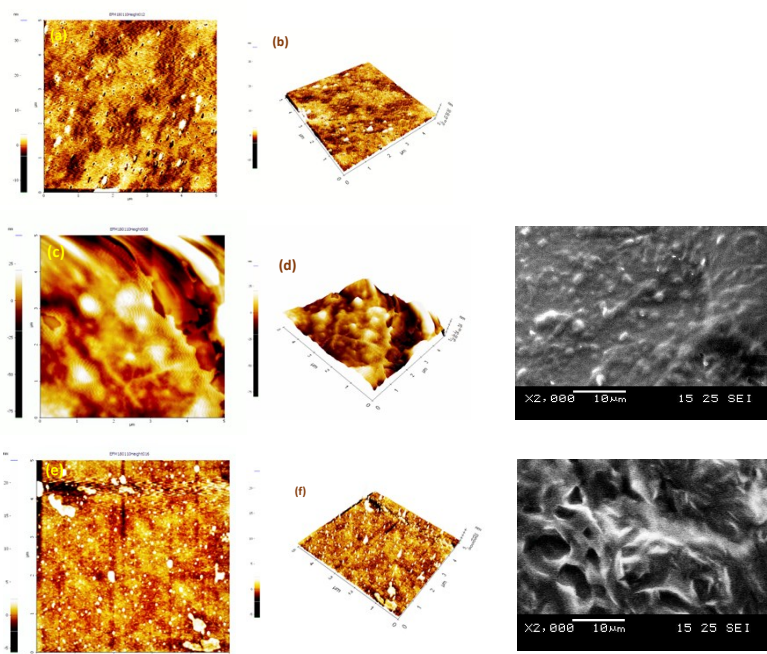


Figure S3. Non-contact mode AFM images of thin films over SiO₂ dielectric layer (a, b) compound **2** (c, d) compound **3** (e, f) compound **4** and SEM images of **3** and **5** (Right).

Computational studies:

Triarylamine molecules with different π extensions were explored theoretically to observe their electronic and charge

transport properties. DFT: B3LYP *ab initio* approach is used to elucidate the structural properties of all molecules. The optimisation of all molecules were done starting from MOPAC and ending with Gaussian at the DFT-B3LYP (6-31g*) level of theory for ground state (S_0). The PBE functional was used to compute the Density of States (DOS), which gave insight into the Fermi levels of the molecules. This depends on density of non-locality states as well by LSDA (low spin density approximation) theory. For comparison *ab-initio* calculations were also done using Gaussian -09 software using B3LYP parameters. The optimized geometry was fed to VASP for further calculations. Precise single crystal parameters of each molecule were predicted successfully using MedeA and used to construct poly crystals. Increment of the molecule to a polycrystalline level was attained by Discovery Studio Viewer and improbable point groups were ruled out. The polymorph prediction calculation were done with 10 most popular space groups such as P21/c, P2, Pbc_a, Pna₂, Cc, Pbc_n and C2 (Cambridge Structural database reference). All the space groups were tried sequentially to monitor interactions and packing measurements and optimized. Dihedral angle between –CHO substituted arm and the other two phenyl conjugated arms is calculated and tabulated. (**Table S2**) Molecules are having dipole moments ranging from 2.0 to 3.8 D. Bond lengths and charges of central nitrogen atom and carbon atoms connected to N atom is also calculated. Generalized representation of molecule is given in **Figure S4**. All stabilised geometrical properties at ground state is given in **Table S2**.

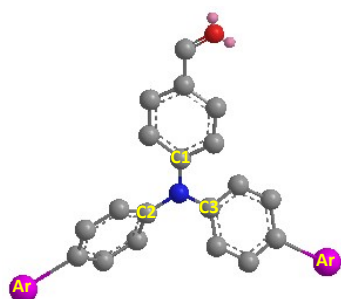


Figure S4. Generalised representation of molecule

Table S2. Geometrical parameters of predicted single crystals **1-8** at ground state S_0

| | Bond length (Å) | | | N | Charges | | | Dihedral angle (°) | Dipole moment (D) |
|---|-----------------|-------|-------|--------|---------|-------|-------|--------------------|-------------------|
| | N-C1 | N-C2 | N-C3 | | C1 | C2 | C3 | | |
| 1 | 1.372 | 1.371 | 1.372 | -1.016 | 0.310 | 0.300 | 0.301 | 149.72 | 2.066 |
| 2 | 1.372 | 1.372 | 1.373 | -0.605 | 0.241 | 0.240 | 0.239 | 145.72 | 2.456 |
| 3 | 1.372 | 1.372 | 1.371 | -0.603 | 0.246 | 0.240 | 0.227 | 151.83 | 2.409 |
| 4 | 1.372 | 1.372 | 1.372 | -0.606 | 0.241 | 0.237 | 0.243 | 145.22 | 2.008 |
| 5 | 1.523 | 1.542 | 1.544 | -0.725 | 0.322 | 0.329 | 0.329 | 139.32 | 2.406 |
| 6 | 1.464 | 1.499 | 1.198 | -0.724 | 0.306 | 0.303 | 0.300 | 145.38 | 3.336 |
| 7 | 1.461 | 1.497 | 1.492 | -0.722 | 0.306 | 0.309 | 0.302 | 153.67 | 3.852 |
| 8 | 1.370 | 1.376 | 1.372 | -0.606 | 0.227 | 0.255 | 0.235 | 144.62 | 2.079 |

All geometrical parameters for molecules **1-8** at ground state S_0 are given in **Table S2**. Packing of all molecules with respect to predicted crystal structures (**Figure S7**) and single crystal parameters given in **Table S3**. Hopping direction and interatomic distance also calculated and projected in **Figure S6** and **Table S4**. The optimised geometry was fed to the MedeA which further predicted the crystal pattern of each molecule using the VASP software at the DFT-PBE-GGA level of theory, suitable for large molecules with predictable material properties. This calculation enabled the estimation of Density of States (DOS) of the molecule in the graphical form (**Figure S5**). In semiconductors the DOS refers to 2D quantum states. Using the Schrodinger's' equation, k-space volume of single state cube (the smallest unit in space to accommodate one electron) was calculated. Compound **3** has maximum volume. The higher value shows more dense packing per unit and smaller 2D state. Quantum dots are a semiconductor crystal that contains electron, hole or electron pair to zero dimensions. Packing distances predicted by these values are visualized. From medea data we arrived at the carrier mobilities of all compound in the range of $10^{-6} \text{ m}^2 \text{ V}^{-1} \text{ s}^{-1}$. The values are given in the table (**Table**

S4) indicates very good value for hopping factor. Molecule **7** has a value of 0.425×10^{-6} , the highest among the series. Obviously, the Fermi levels are also very high for the molecule and outrageous HOMO-LUMO distribution is also discussed. This molecule possesses largest value in the nearest possible pathway predicted by MedeA for the Space group P21.

Table S3. Crystal structure and lattice parameters at ground level S_0

| | Type | Sides | | | Angles | | | |
|----------|-----------------------------|-------|-------|------|----------|---------|----------|-------|
| | | A | B | C | α | β | γ | μ |
| 1 | Triclinic (CC) | 15.05 | 13.35 | 6.46 | 93.13 | 89.24 | 89.00 | 2.066 |
| 2 | Triclinic (PNA-21) | 25.45 | 16.15 | 5.89 | 89.62 | 88.09 | 89.90 | 2.456 |
| 3 | Triclinic (P-21) | 28.07 | 17.79 | 5.80 | 87.81 | 91.33 | 90.06 | 2.409 |
| 4 | Triclinic (P-1) | 19.84 | 14.96 | 5.97 | 89.20 | 89.54 | 90.15 | 2.008 |
| 5 | Triclinic (P-21-C) | 20.28 | 15.74 | 6.11 | 89.55 | 89.4 | 90.32 | 2.406 |
| 6 | Triclinic (P-1) | 24.00 | 16.64 | 6.41 | 90.72 | 89.80 | 90.70 | 3.336 |
| 7 | Triclinic (P-21) | 20.53 | 16.82 | 9.25 | 90.09 | 89.78 | 90.07 | 3.858 |
| 8 | Triclinic (P-1) | 23.06 | 16.14 | 6.48 | 90.20 | 88.44 | 89.71 | 2.079 |

Orbital overlap leading to efficient charge transfer is also a key concept while orienting the structure. HOMO's and LUMO's were keenly observed and their interacting distances maximum was chosen for the hopping values. It was possible to choose good number of hopping values but in given crystal structure only a few were considered. Orbital overlaps have been excluded from figure to present a simplified outlook.

Table S4. Interatomic distance, band gap and mobility of compounds **1-8**

| | Volume | Density | Interatomic distance(Å) | DOS band gap(eV) DFT GGA-PBE | Charge carrier mobility ($m^2V^{-1}s^{-1}$) |
|----------|---------|---------|-------------------------|---------------------------------|--|
| 1 | 1297.08 | 0.672 | H-I 2.112 / N-H 3.115 | 2.1088 | 0.146×10^{-6} |
| 2 | 2421.71 | 0.360 | O-H 9.557 / N-H 6.525 | 2.0072 | 0.089×10^{-6} |
| 3 | 2896.79 | 0.331 | O-H 3.785 / N-O 2.861 | 2.0148 | 0.081×10^{-6} |
| 4 | 1775.72 | 0.409 | S-N 1.529 / O-H 6.985 | 1.9932 | 0.097×10^{-6} |
| 5 | 1951.78 | 0.362 | N-O 2.904 / H-O 4.191 | 2.0185 | 0.110×10^{-6} |
| 6 | 2561.22 | 0.315 | H-O 4.742 / N-H 6.570 | 1.9872 | 0.141×10^{-6} |
| 7 | 3199.29 | 0.268 | N-O 9.135 / O-H 6.284 | 1.4841 | 0.425×10^{-6} |
| 8 | 2411.98 | 0.387 | H-F 11.273 / N-F 11.773 | 2.0811 | 0.140×10^{-6} |

Qualitative representation of HOMO and LUMO were visualized using Gaussview and Chemcraft

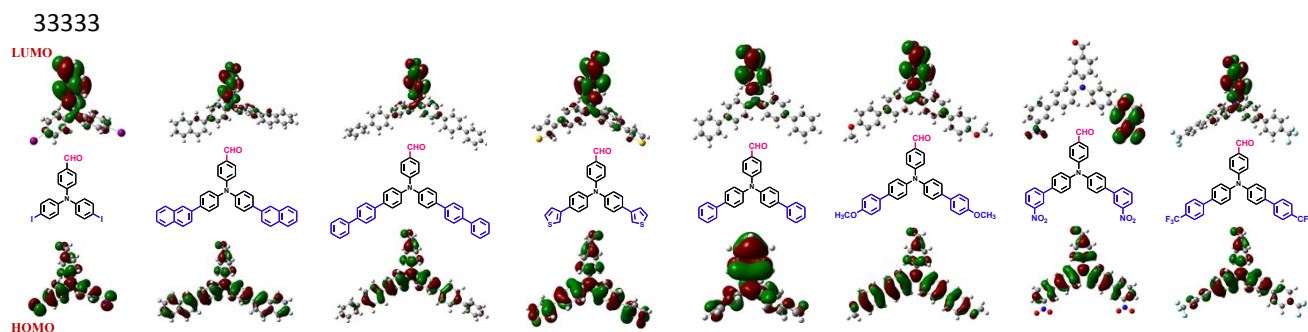
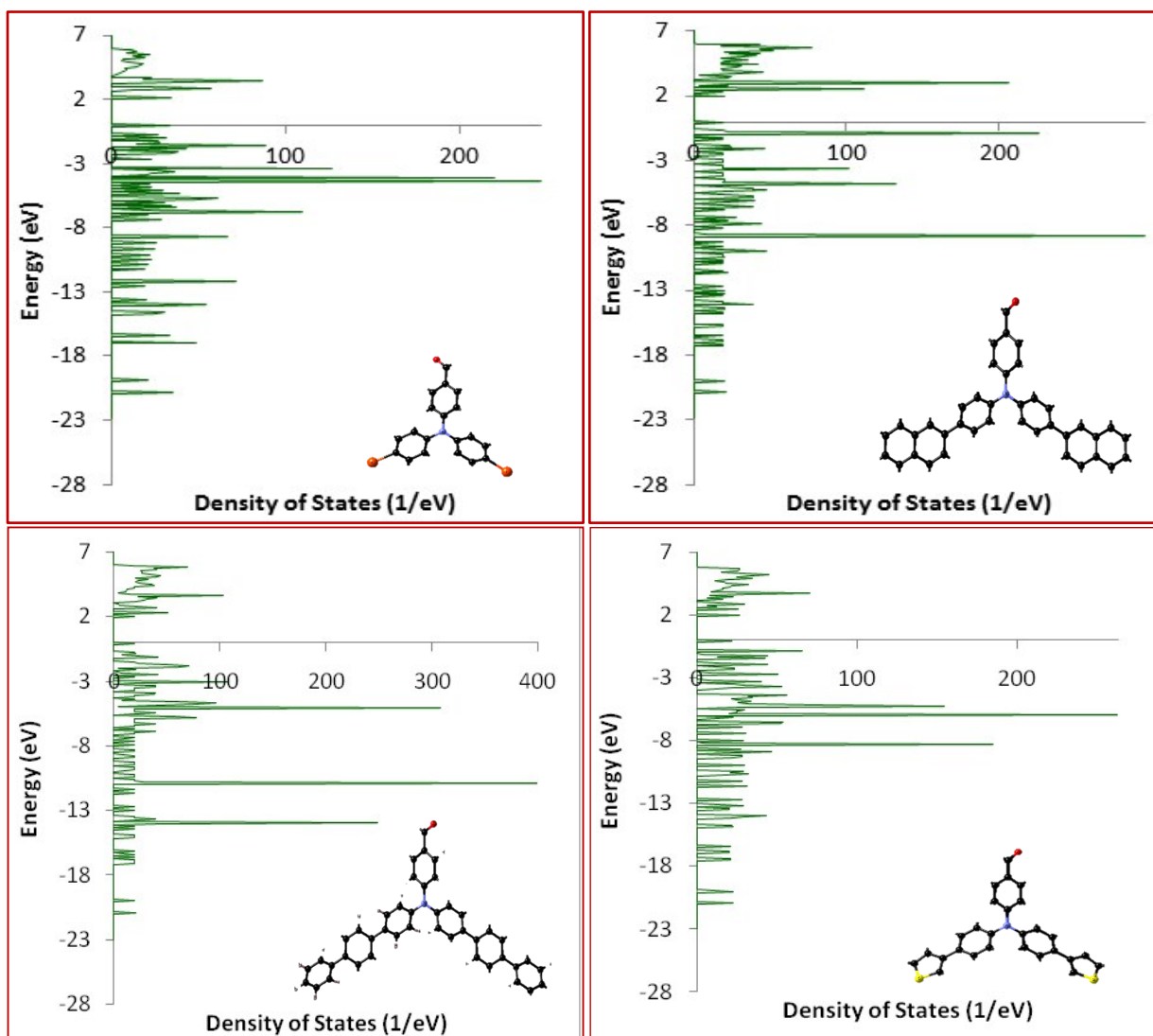


Figure S5. Spatial distributions of FMOs of compounds **1-8**

Electron density in HOMO is distributed all over triarylamine donor moiety and LUMO towards the acceptor moiety. Figure 4 shows FMOs of all the compounds. Molecule **7** with NO₂ group has outrageous distribution than other molecules. Nitro group increases electron affinity and as the stabilization effect LUMO is located over NO₂ than on HOMO.ⁱⁱⁱ From an analysis of all the HOMOs and LUMOs of the molecules, it is inferred that all the molecules have very high percentage of the HOMO's on the central triarylamine moiety and less percentage of the LUMO's on the derivative sides (**Figure S5**). This substantiate the π extensions are introduced without affecting the peculiarity of orbitals. **Table 2** shows that predicted band gap values (DFT-B3LYP) are in agreement with experimental value. But values predicted by VASP at the PBA levels varies because of fermi level added in crystalline structure.

The DOS band gap values predicted by MedeA ranges from 1.484 eV to 2.108 eV (**Table S4**). A good spread of the Fermi levels shows the possible states the electron can move. Here, compound **3** found to have the highest fermi level and lowest band gap among all. And it is expected to have good physical properties when constituted to poly crystalline level. Compounds **2** and **5** shows moderate fermi level. In all the molecules deviation is negligible and can be concluded to possess very good electronic property. .



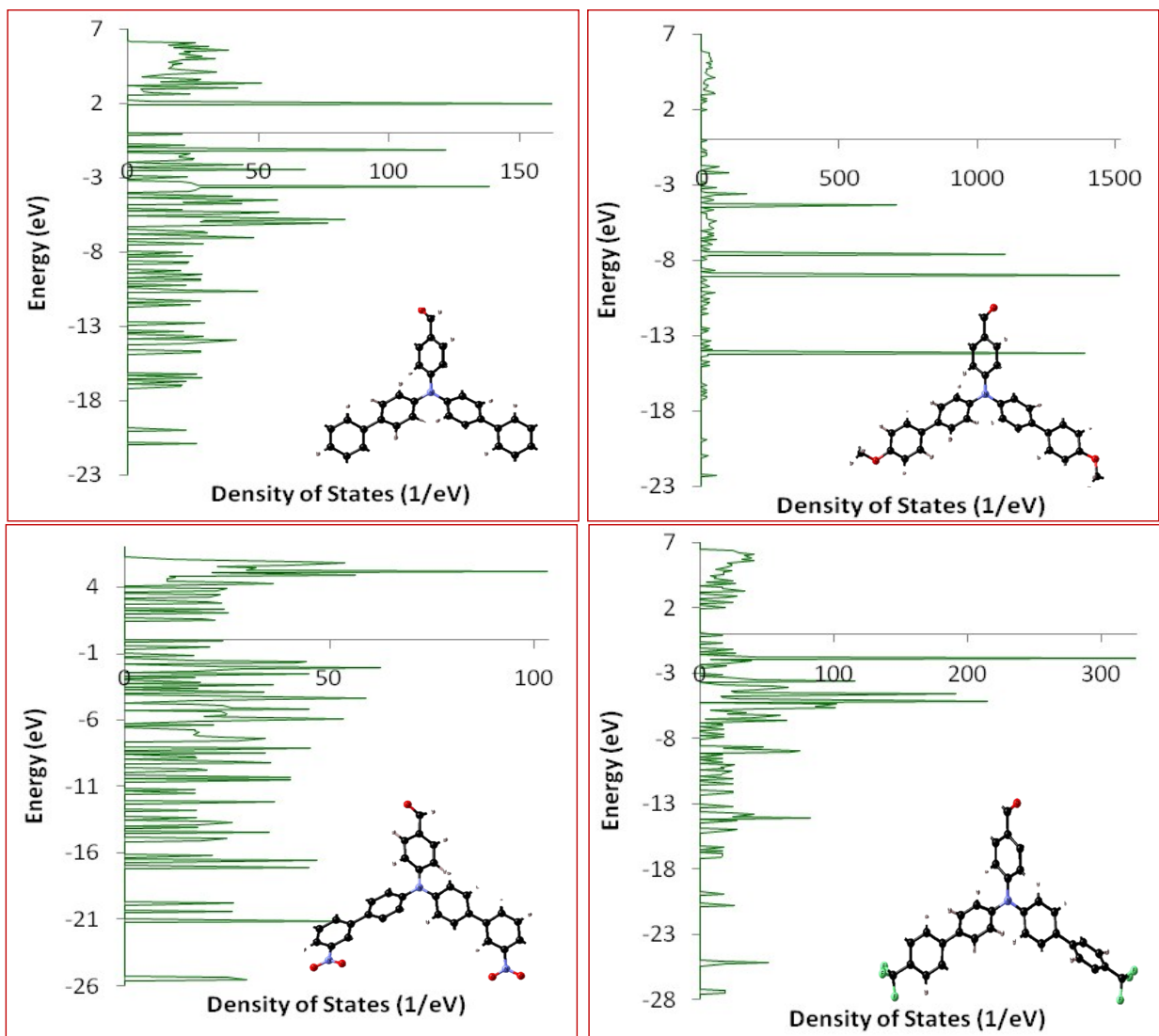
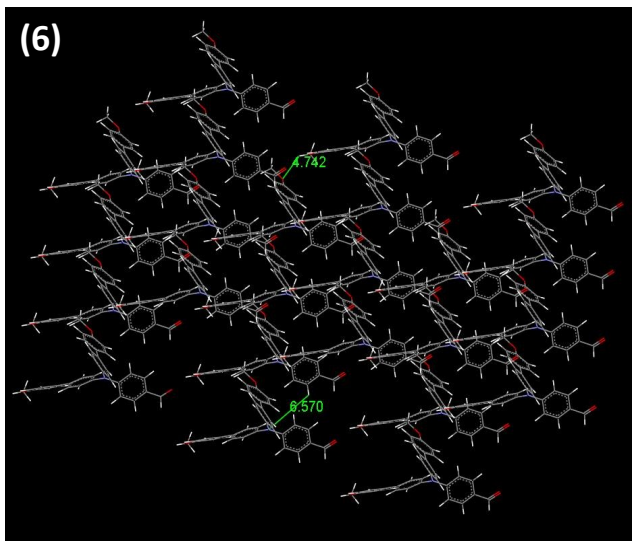
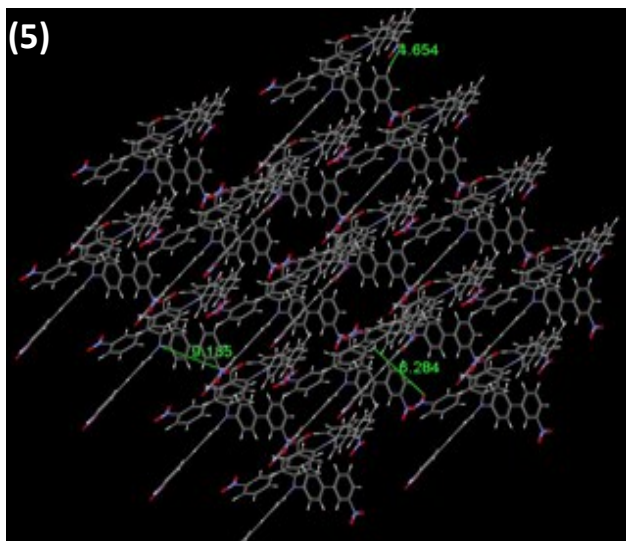
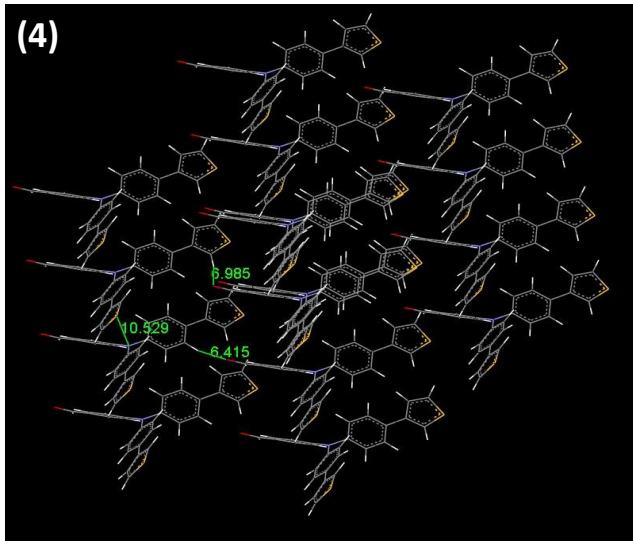
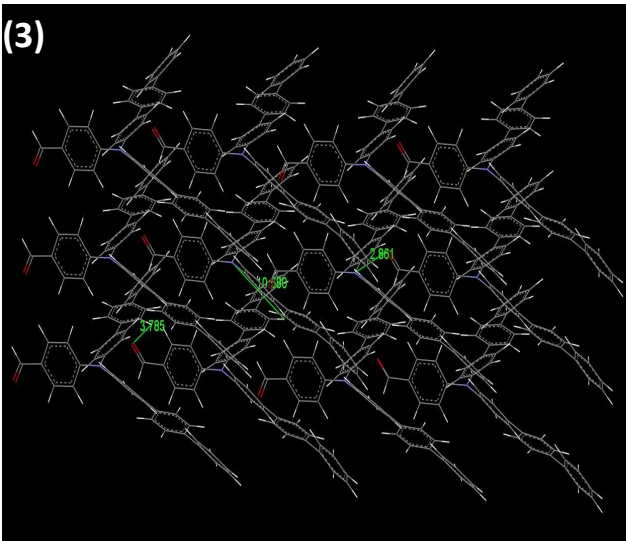
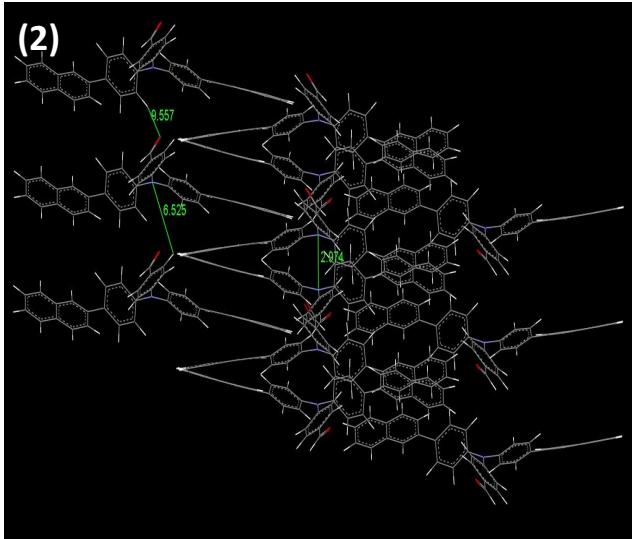
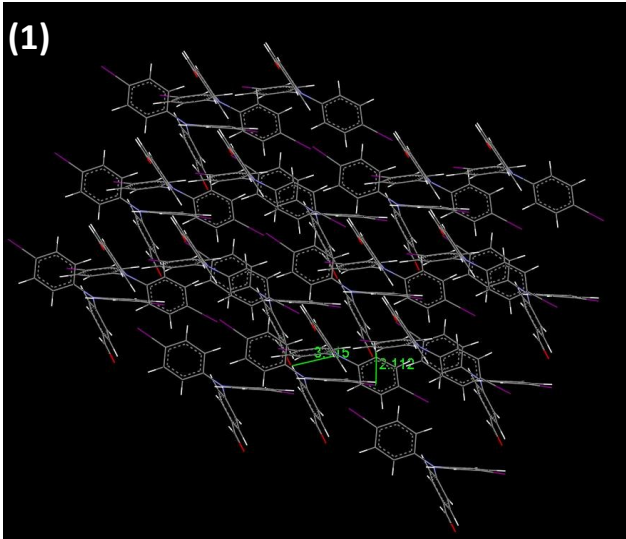


Figure S6. Density of States graphs of compounds 1-8 (Inset is stabilized ground state structures)



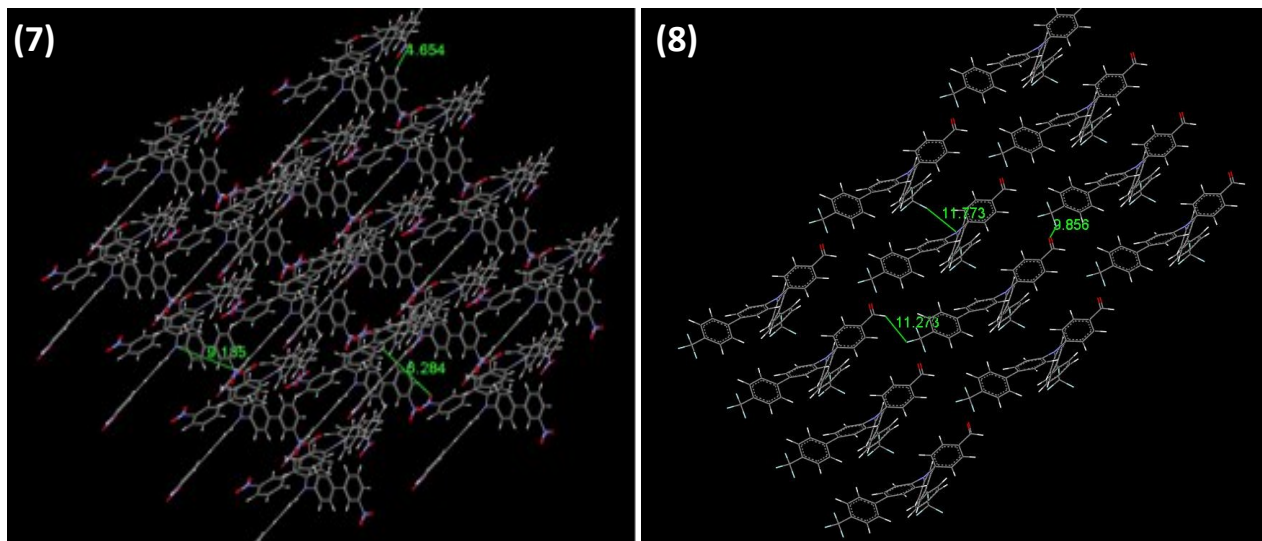
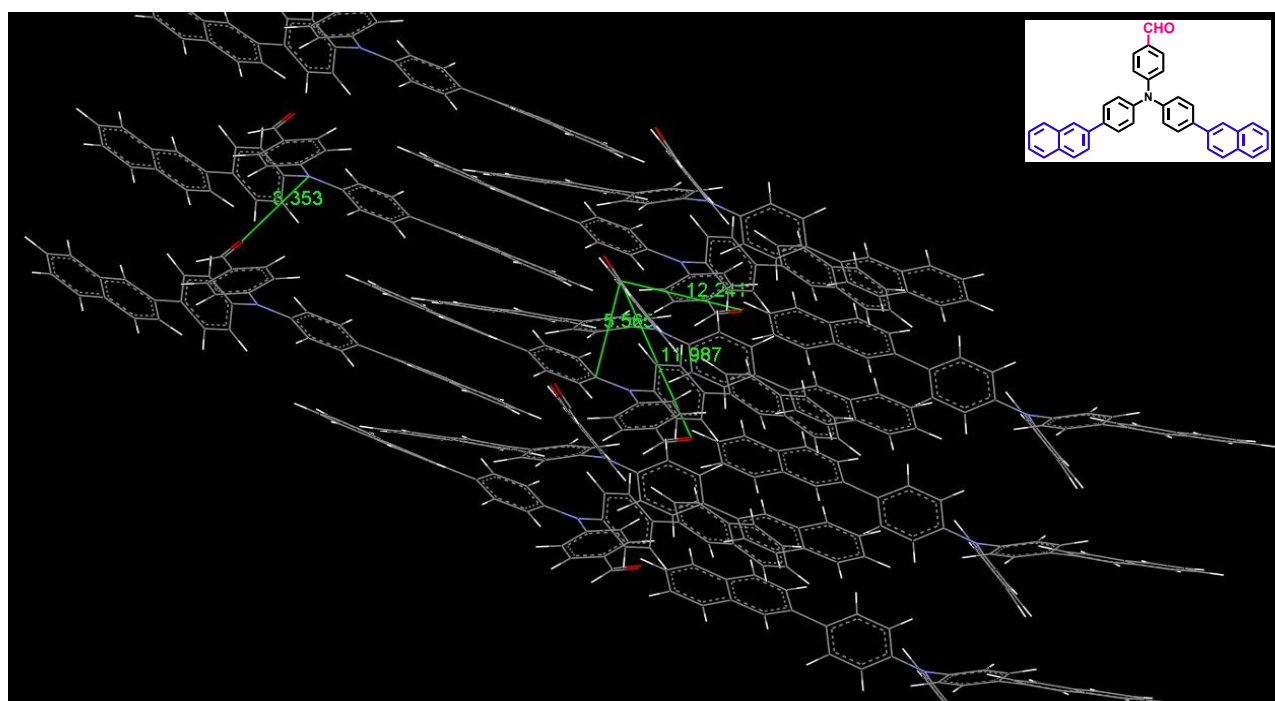


Figure S7. Polymorph predictions at polycrystalline level



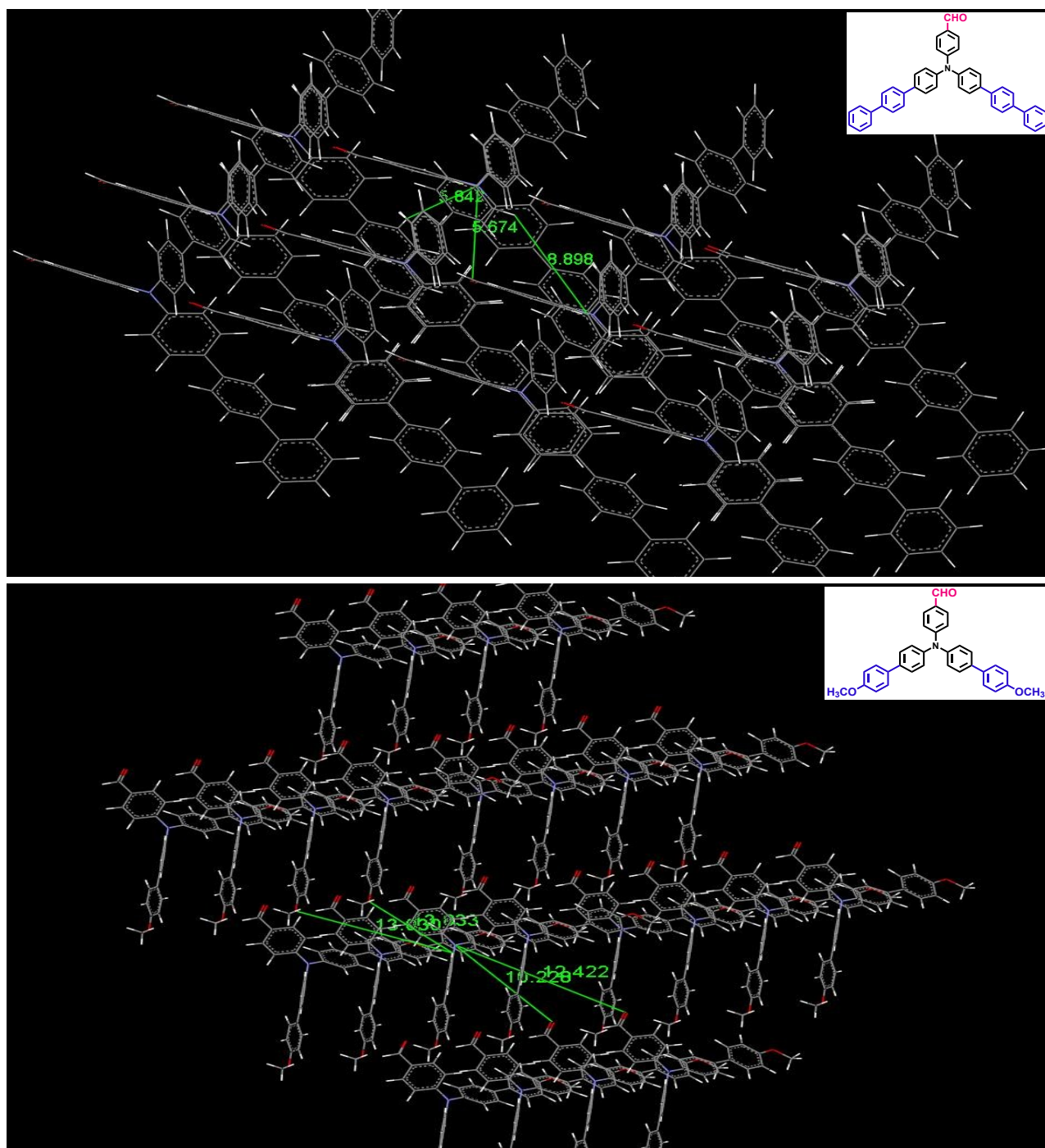
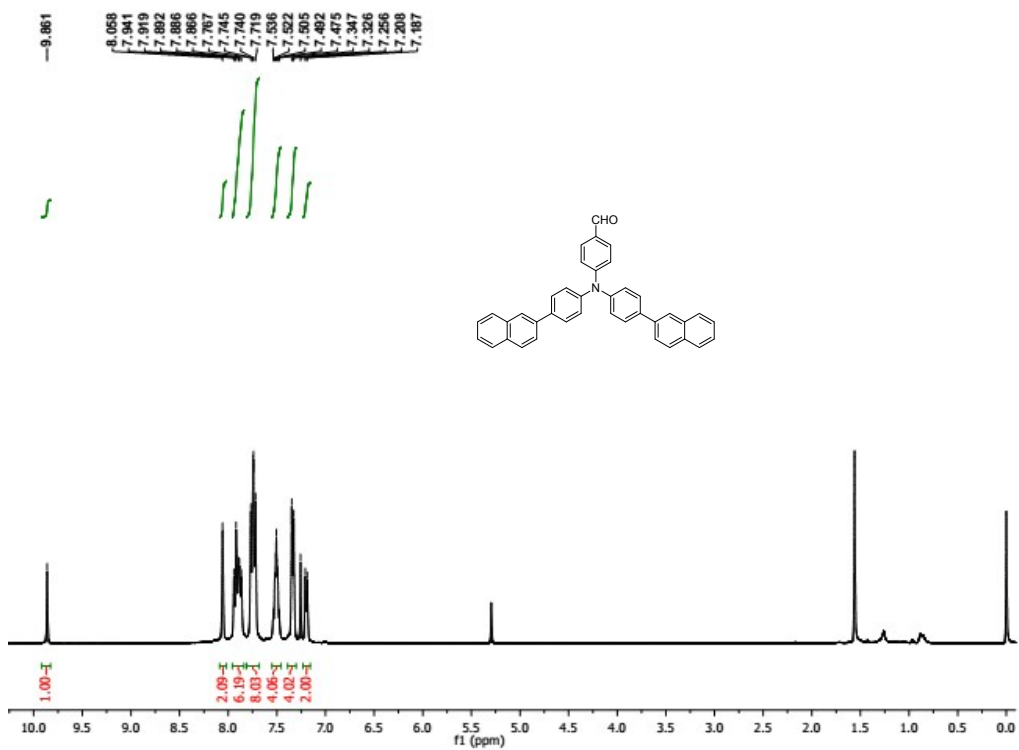
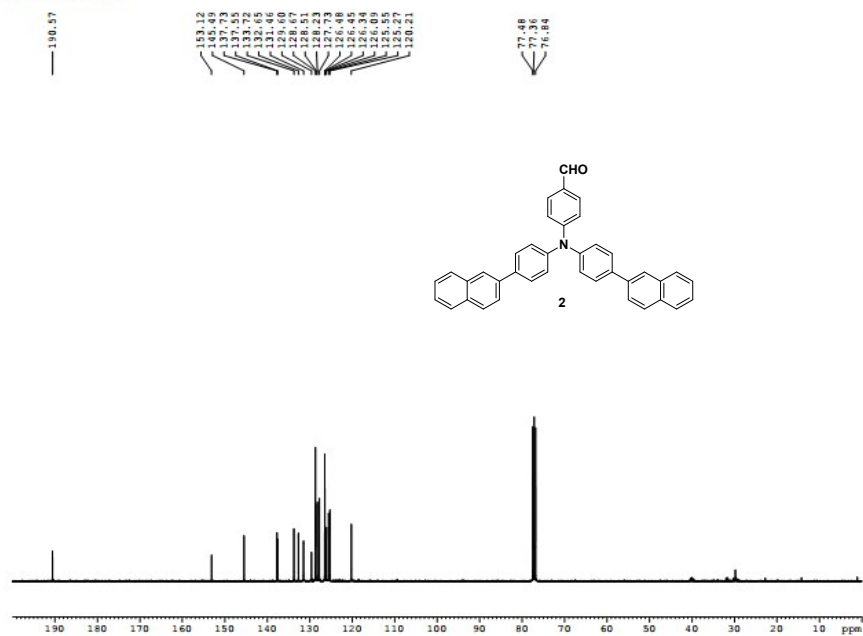


Figure S8. Hopping distance prediction at polycrystalline packing.



DR15 DHEEPIKA



```

Current Data Parameters
NAME      DR15
EXPNO    1
PROCNO   1

F2 - Acquisition Parameters
Date_    20160831
Time     11:30
SYSTEM
PROBHD   5 mm PABBO BB-
PULPROG  zgpg30
TD        65536
SOLVENT   CDCl3
NS        1024
DS        4
SWH       24038.461 Hz
FIDRES    0.360796 Hz
AQ         1.3031988 sec
RG         190.62
MF         10.800 usec
ME         6.50 usec
TE         300.2 K
D1         2.00000000 sec
d11        0.03000000 sec

===== CHANNEL f1 =====
NUC1       13C
P1         8.15 usec
PLM1      05.40000153 W
SFO1      100.6218293 MHz

===== CHANNEL f2 =====
CPDPRG2   waltz16
NUC2
PCPD2     90.00 usec
PLM2      11.00000000 W
SFO2      0.24700000 W
PLM3      0.20048000 W
SFO3      400.1316005 MHz

F2 - Processing parameters
SI         32768
SF         100.6127490 MHz
RG         0
SSB        0
LB         1.00 Hz
GB         0
PC         1.40
  
```

Figure S9. ¹H NMR and ¹³C NMR spectra of compound 2

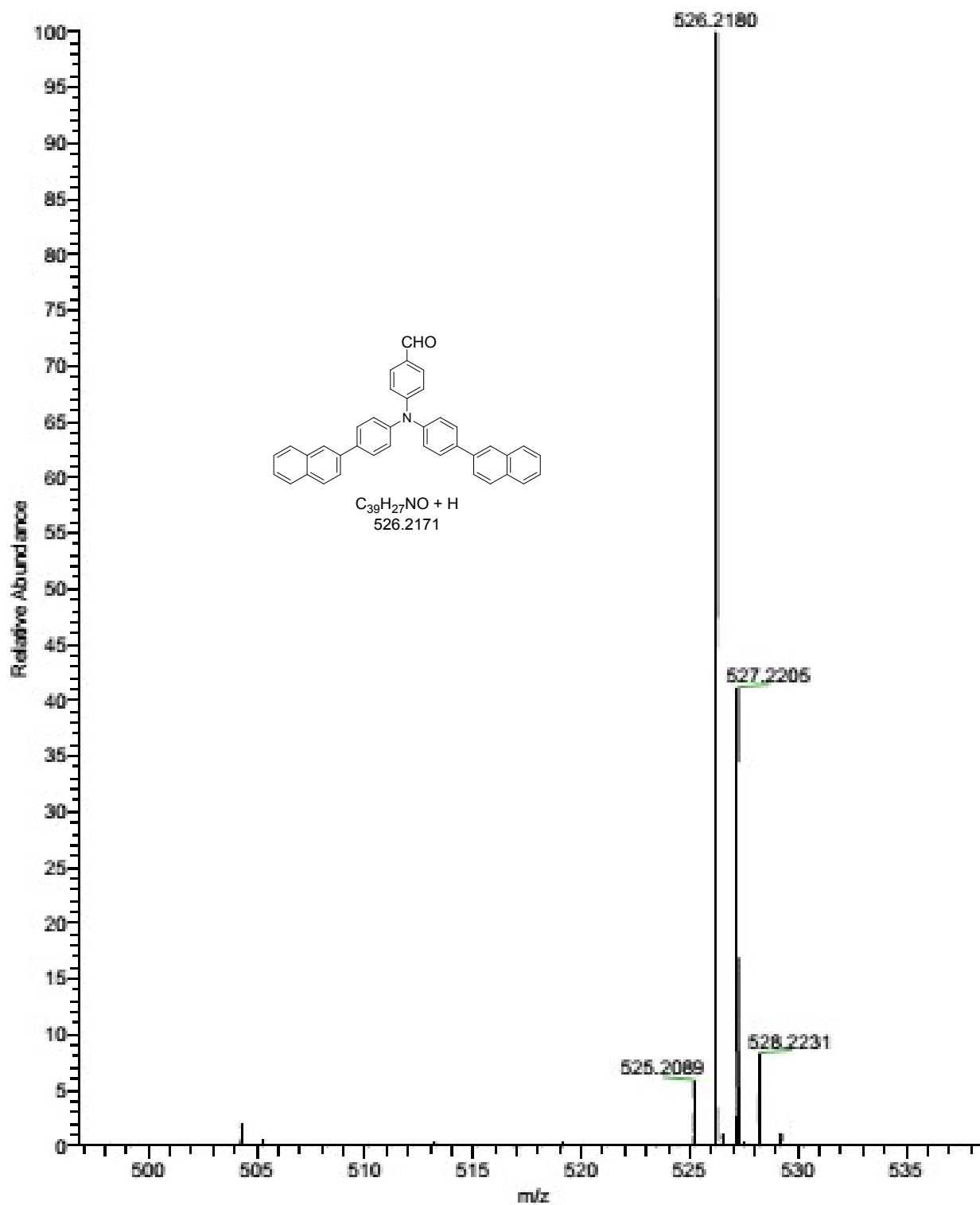


Figure S10. HR-Mass spectra of compound 2

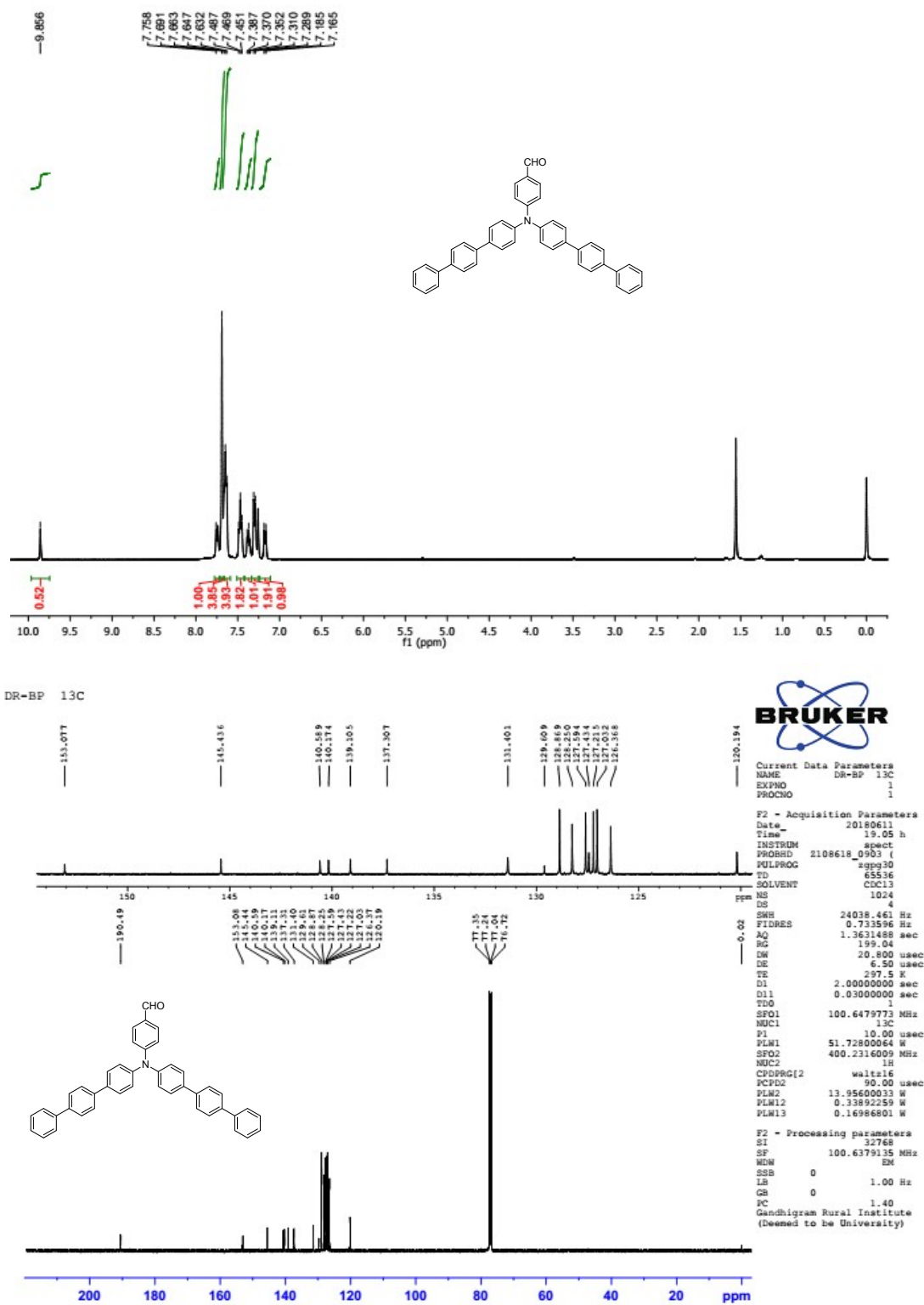


Figure S11. ¹H NMR and ¹³C NMR spectra of compound 3

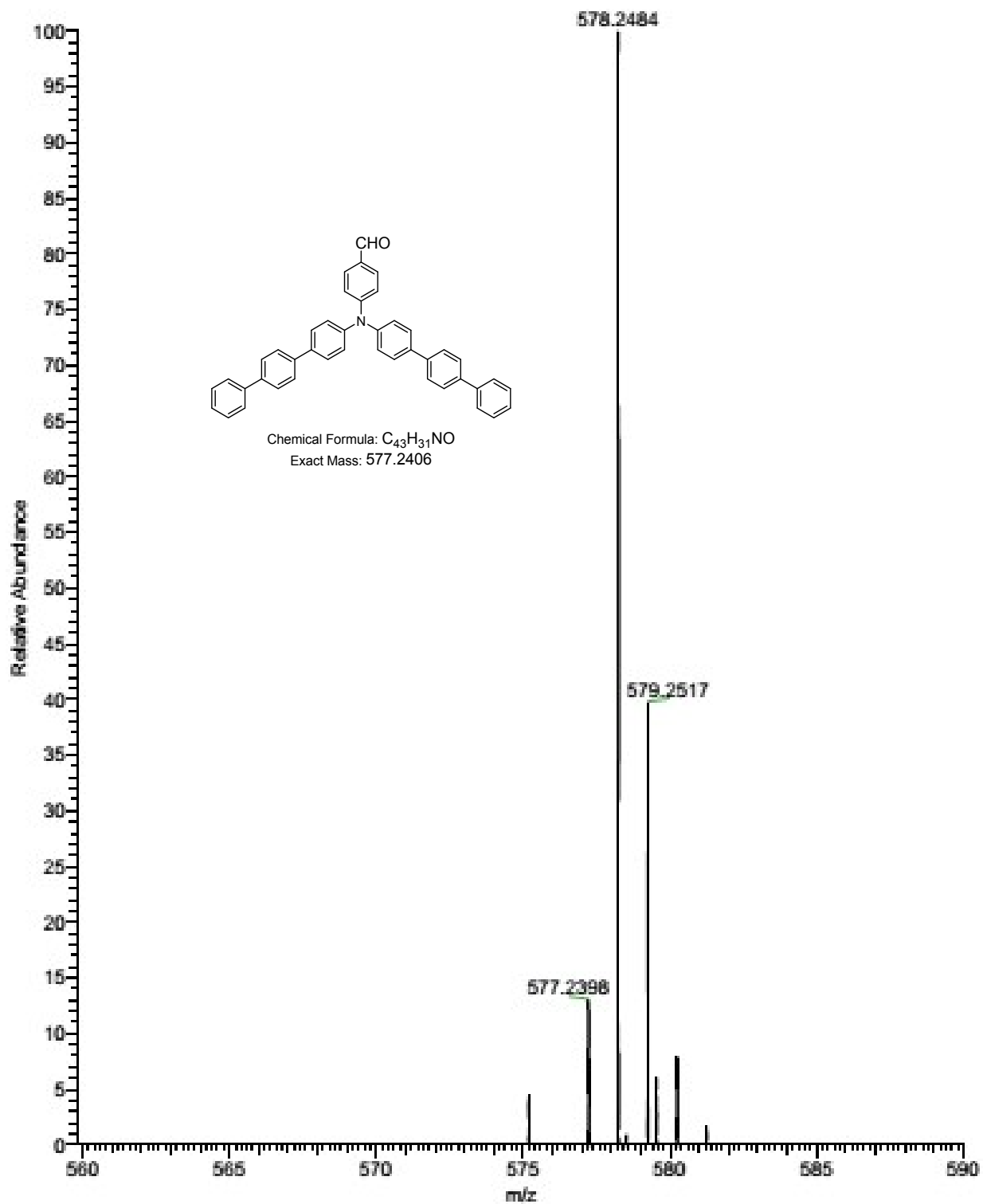
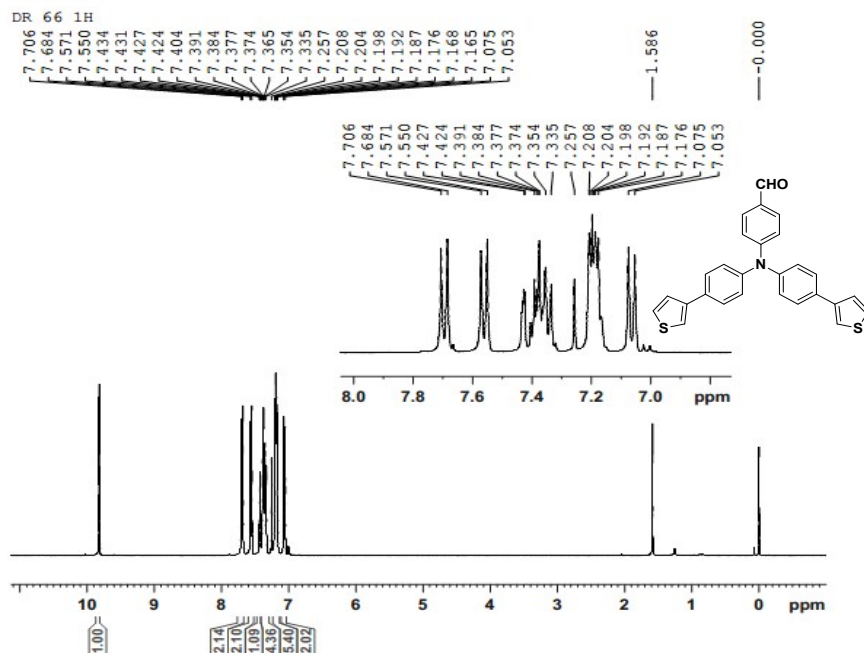


Figure S12. HR-Mass spectra of compound 3

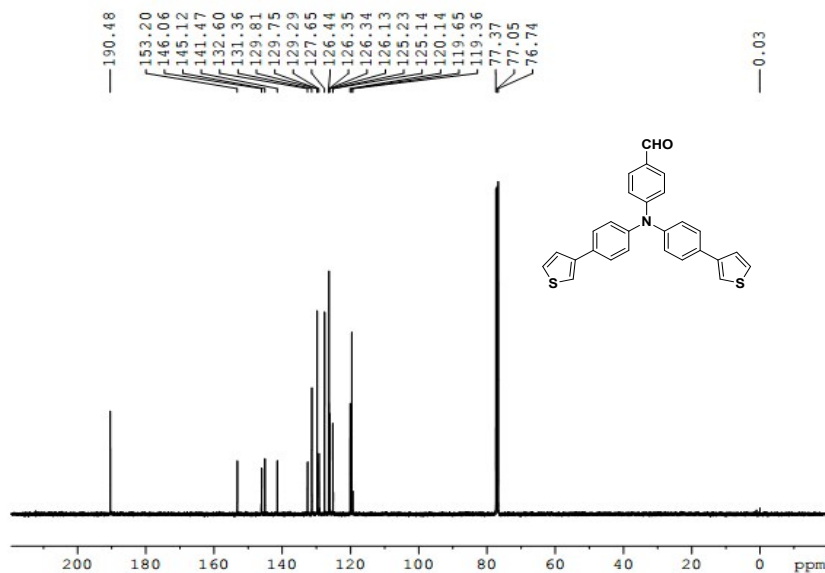


Current Data Parameters
 NAME DR 66 1H
 EXPNO 1
 PROCNO 1

F2 - Acquisition Parameters
 Date 20170418
 Time 13.36 h
 INSTRUM spect
 PROBRD z108618_0903
 PULPROG zg30
 TD 65536
 SOLVENT CDCl3
 NS 16
 DS 2
 SWH 8012.820 Hz
 FIDRES 0.244532 Hz
 AQ 4.0894465 sec
 RG 160.97
 DW 62.400 usec
 DE 6.50 usec
 TE 295.8 K
 D1 1.00000000 sec
 TDO
 SFO1 400.2324714 MHz
 NUC1 1H
 P1 14.00 usec
 PLW1 13.95600033 W

F2 - Processing parameters
 SI 65536
 SF 400.2300110 MHz
 WDW EM
 SSB 0
 LB 0.30 Hz
 GB 0
 PC 1.00

DR-66 13C



Current Data Parameters
 NAME DR-66 13C
 EXPNO 1
 PROCNO 1

F2 - Acquisition Parameters
 Date 20170921
 Time 12.46 h
 INSTRUM spect
 PROBRD z108618_0903
 PULPROG zgpg30
 TD 65536
 SOLVENT CDCl3
 NS 660
 DS 4
 SWH 24038.461 Hz
 FIDRES 0.733596 Hz
 AQ 1.3631488 sec
 RG 199.04
 DW 20.800 usec
 DE 6.50 usec
 TE 296.7 K
 D1 2.00000000 sec
 D11 0.03000000 sec
 TDO
 SFO1 100.6479773 MHz
 NUC1 13C
 P1 10.00 usec
 PLW1 51.72800064 W
 SFO2 400.2316009 MHz
 NUC2 1H
 CPDPRG2 waltz16
 PCPD2 90.00 usec
 PLW2 13.95600033 W
 PLW12 0.33892259 W
 PLW13 0.16986801 W

F2 - Processing parameters
 SI 32768
 SF 100.6379135 MHz
 WDW EM
 SSB 0
 LB 1.00 Hz
 GB 0
 PC 1.40

Figure S13. ¹HNMR and ¹³CNMR spectra of compound 4

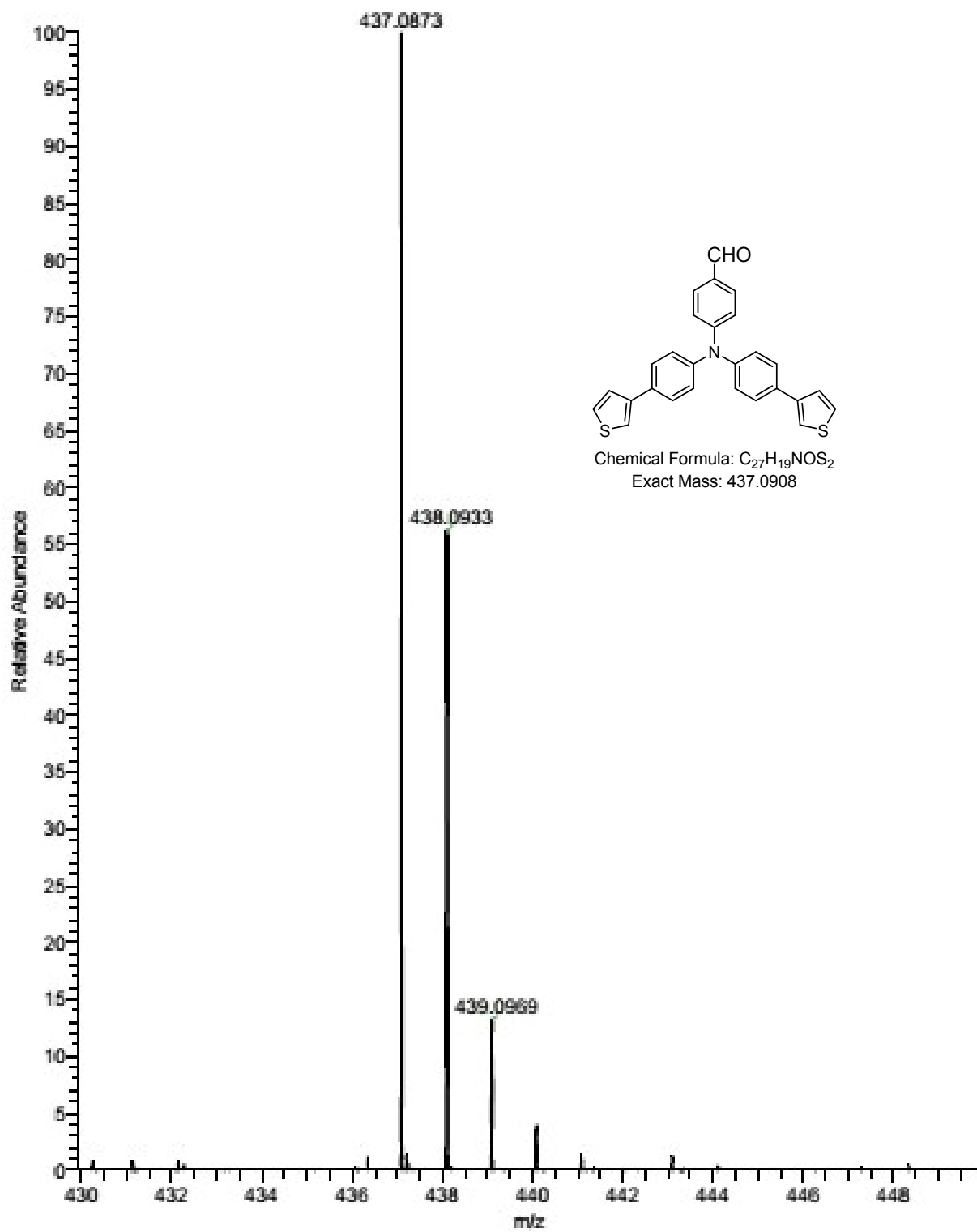
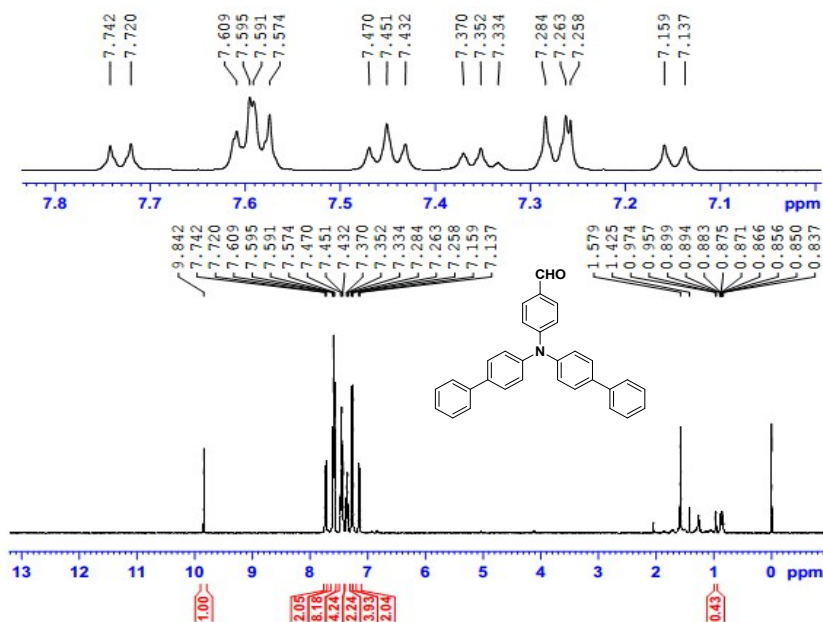


Figure S14. HR-Mass spectra of compound 4

DR-1 1H

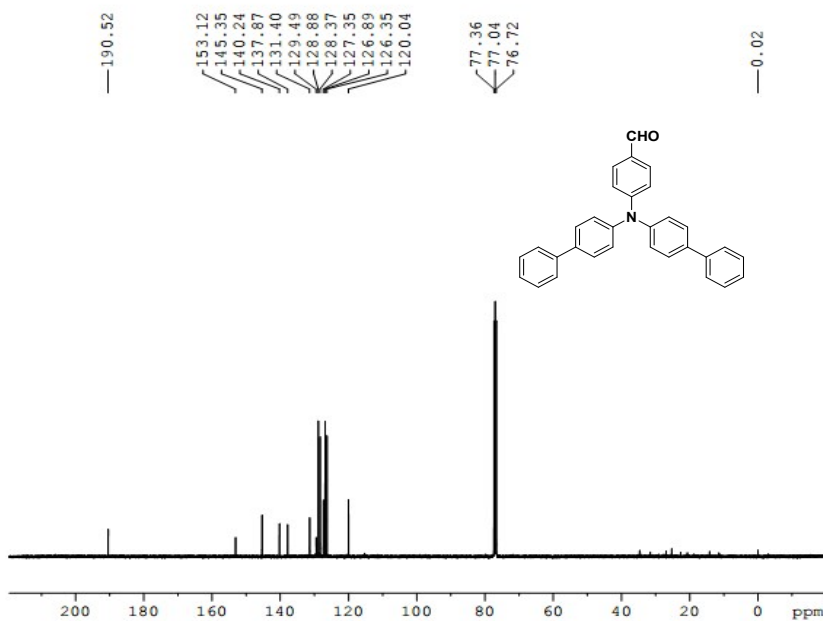


Current Data Parameters
 NAME DR-1 1H
 EXPNO 1
 PROCNO 1

F2 - Acquisition Parameters
 Date 20170803
 Time 14.45 h
 INSTRUM spect
 PROBHD z108618_0903 (i)
 PULPROG zg30
 TD 65536
 SOLVENT CDCl3
 NS 16
 DS 2
 SWH 8012.820 Hz
 FIDRES 0.244532 Hz
 AQ 4.0894465 sec
 RG 179.3
 DW 62.400 usec
 DE 6.50 usec
 TE 294.8 K
 D1 1.00000000 sec
 TDO
 SFO1 400.2324714 MHz
 NUC1 1H
 P1 14.00 usec
 PLW1 13.95600033 W

F2 - Processing parameters
 SI 65536
 SF 400.2300196 MHz
 MDW EM
 SSB 0
 LB 0.30 Hz
 GB 0
 PC 1.00

DR-1 13C



Current Data Parameters
 NAME DR-1 13C
 EXPNO 1
 PROCNO 1

F2 - Acquisition Parameters
 Date 20170904
 Time 14.50 h
 INSTRUM spect
 PROBHD z108618_0903 (i)
 PULPROG zgpg30
 TD 65536
 SOLVENT CDCl3
 NS 600
 DS 4
 SWH 24038.461 Hz
 FIDRES 0.733596 Hz
 AQ 1.3631488 sec
 RG 199.04
 DW 20.800 usec
 DE 6.50 usec
 TE 296.1 K
 D1 2.00000000 sec
 D11 0.03000000 sec
 TDO 1
 SFO1 100.6479773 MHz
 NUC1 13C
 P1 10.00 usec
 PLW1 51.72800064 W
 SFO2 400.2316009 MHz
 NUC2 1H
 CPDPRG[2] waltz16
 PCPD2 90.00 usec
 PLW2 13.95600033 W
 PLW12 0.33892259 W
 PLW13 0.16986801 W

F2 - Processing parameters
 SI 32768
 SF 100.6379135 MHz
 MDW EM
 SSB 0
 LB 1.00 Hz
 GB 0
 PC 1.40

Figure S15. ¹H NMR and ¹³C NMR spectra of compound 5

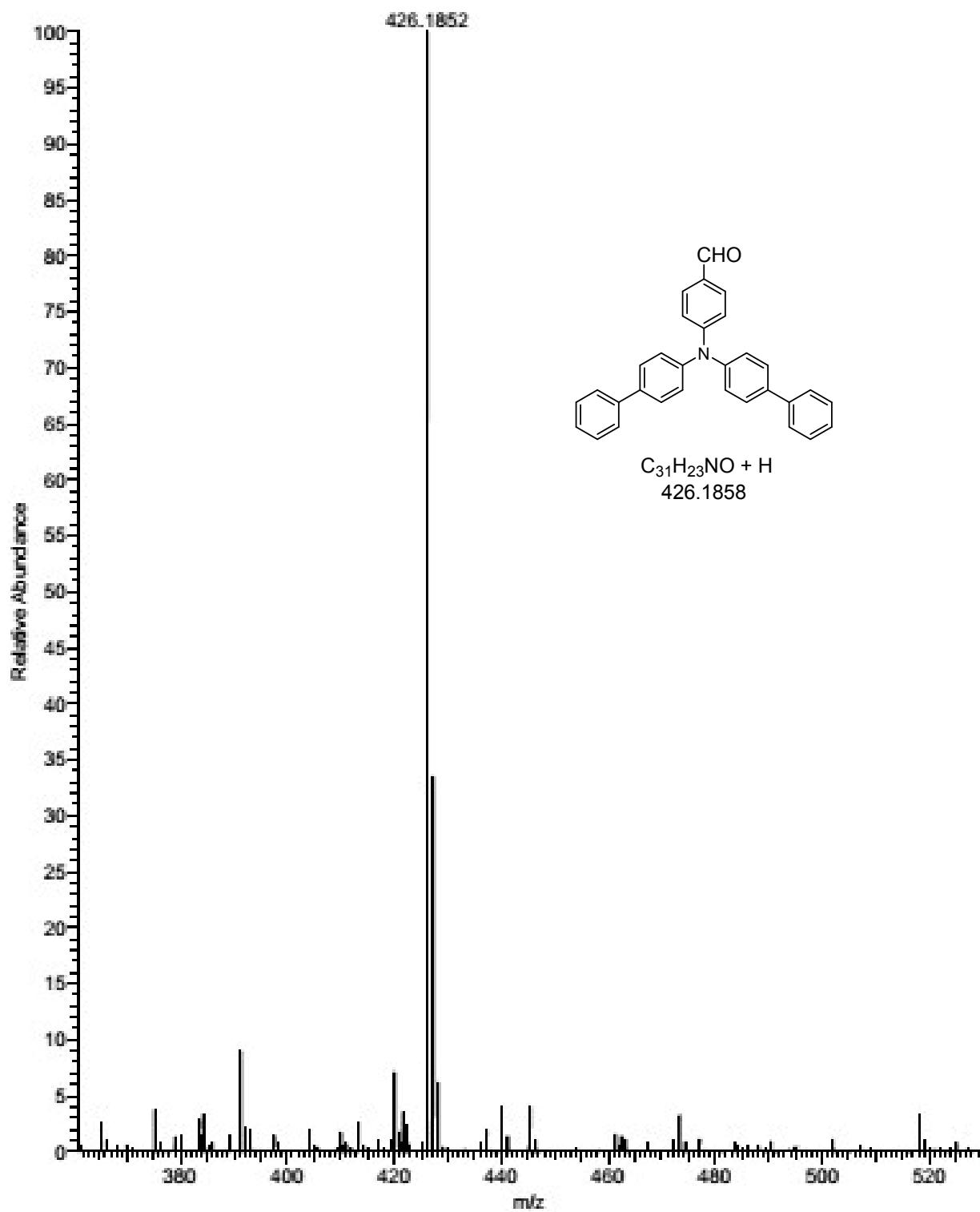


Figure S16. HR-Mass spectra of compound 5

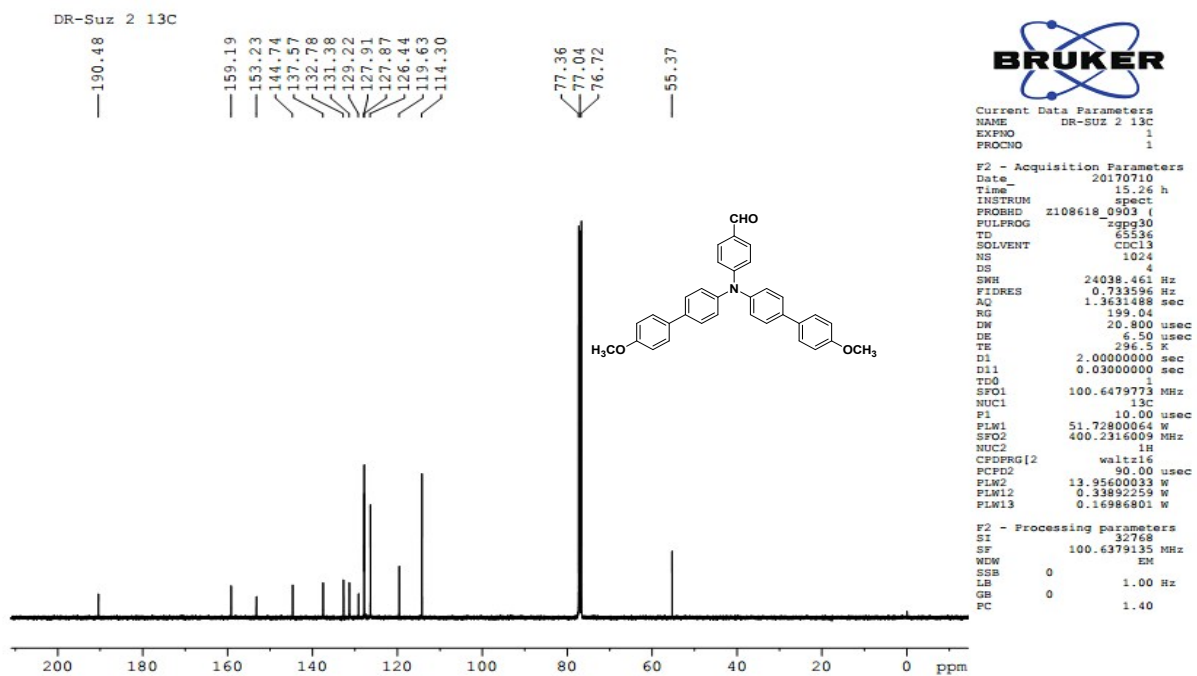
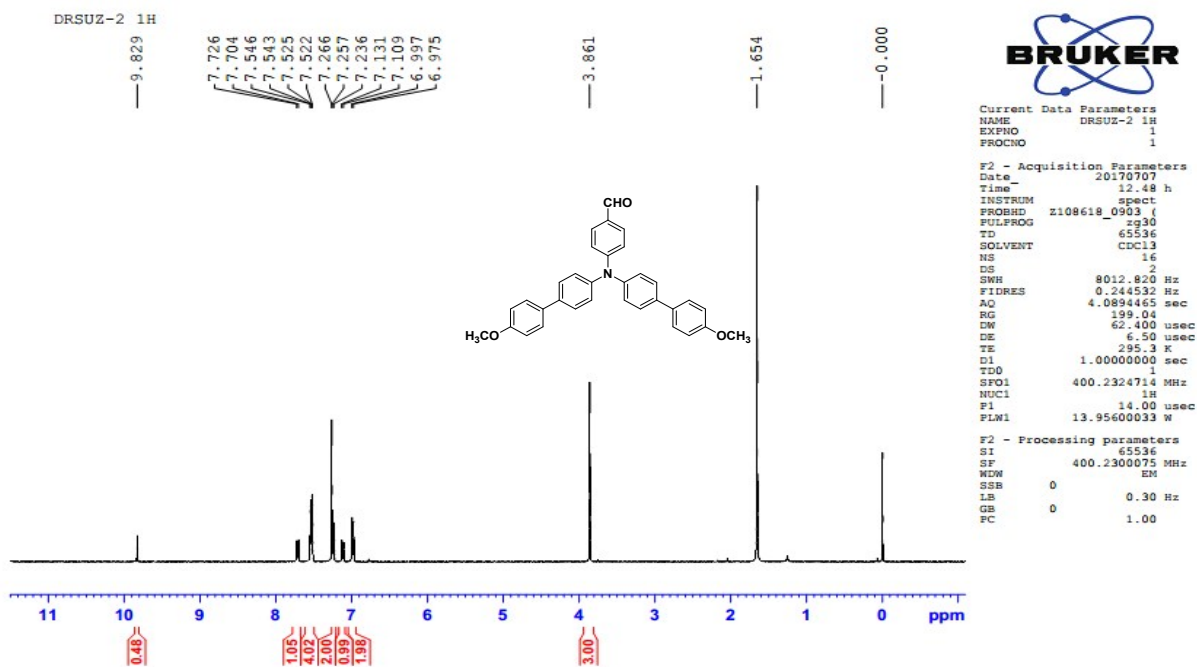


Figure S17. ¹HNMR and ¹³CNMR spectra of compound 6

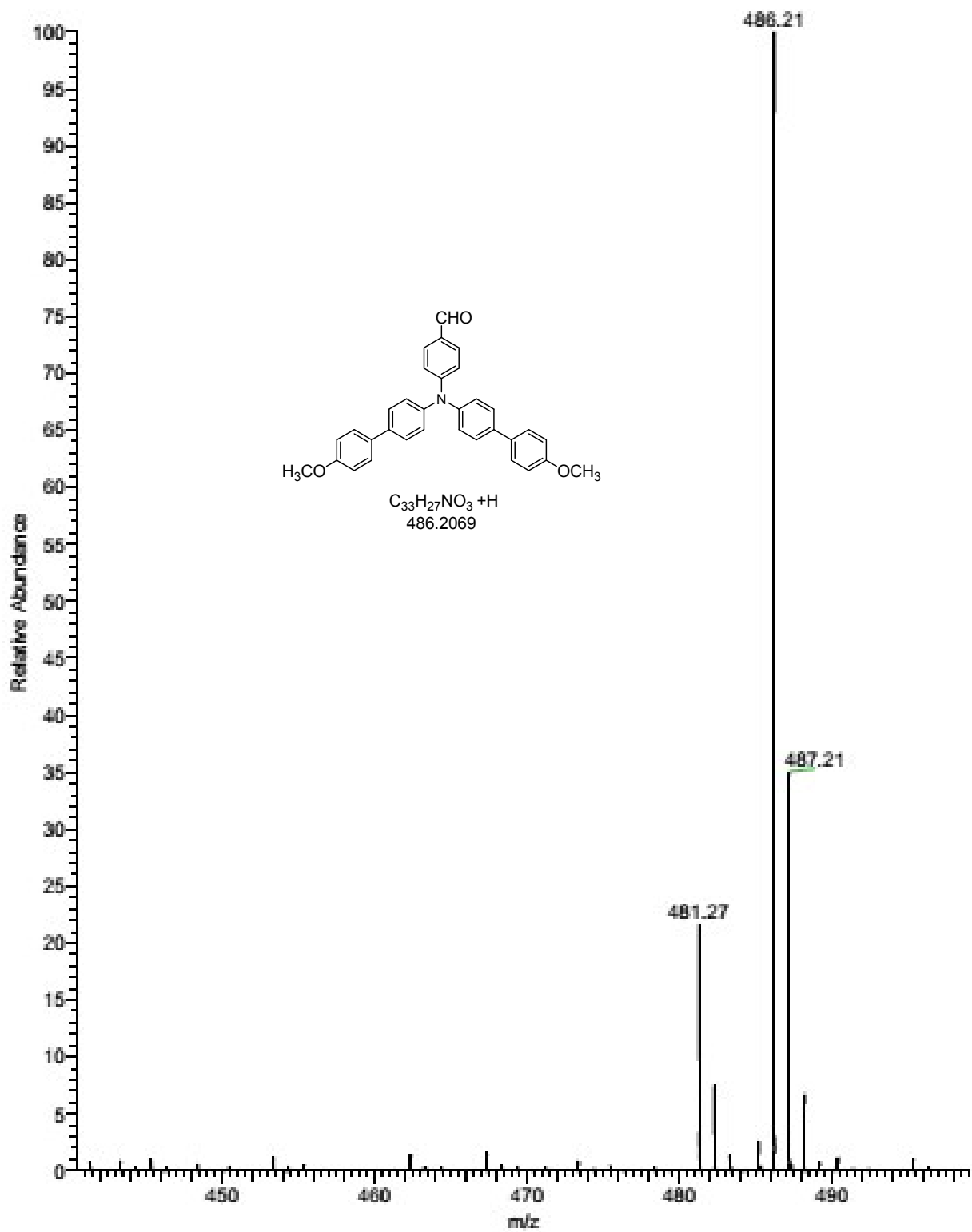
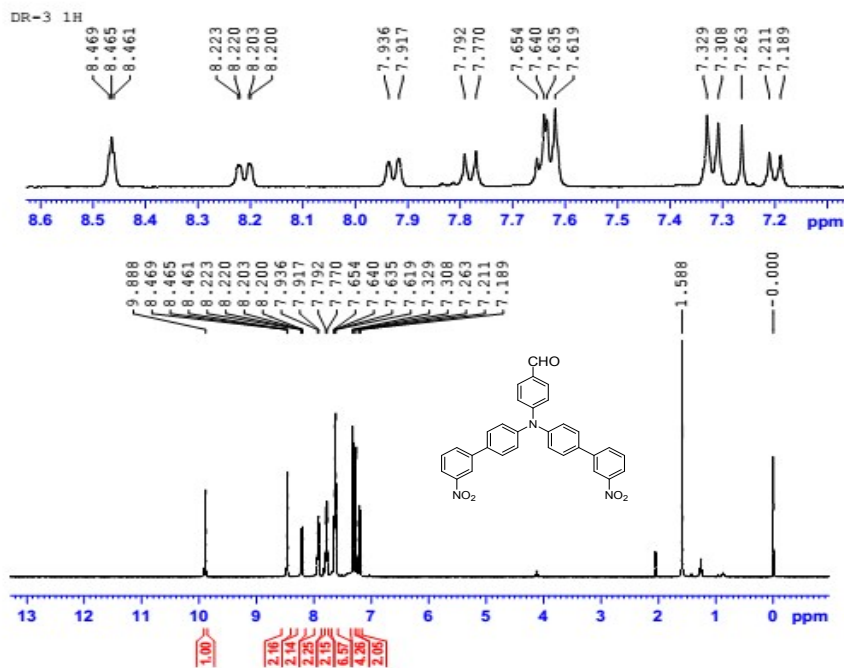


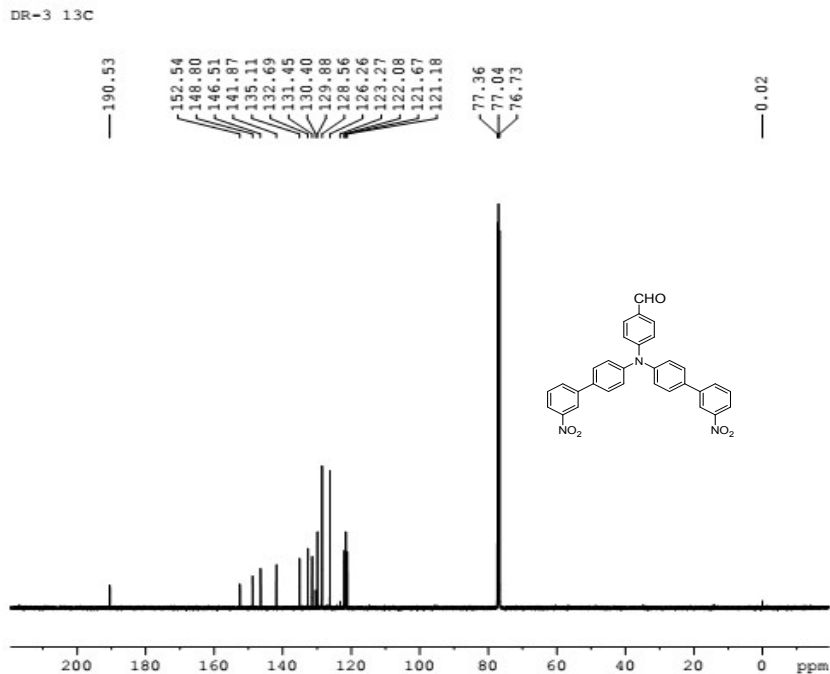
Figure S18. HR-Mass spectra of compound 6



Current Data Parameters
 NAME DR-3 1H
 EXPNO 1
 PROCNO 1

F2 - Acquisition Parameters
 Date_ 20170803
 Time_ 14.51 h
 INSTRUM spect
 PROBRD 2108618_0903 ()
 PULPROG zg30
 TD 65536
 SOLVENT CDCl3
 NS 16
 DS 2
 SWH 8012.820 Hz
 FIDRES 0.244532 Hz
 AQ 4.0894465 sec
 RG 199.04
 DM 62.400 usec
 DE 6.50 usec
 TE 294.8 K
 D1 1.0000000 sec
 TDO
 SFO1 400.2324714 MHz
 NUC1 1H
 P1 14.00 usec
 PLW1 13.95600033 W

F2 - Processing parameters
 SI 65536
 SF 400.2300085 MHz
 WDW EM
 SSB 0
 LB 0.30 Hz
 GB 0
 PC 1.00



Current Data Parameters
 NAME DR-3 13C
 EXPNO 1
 PROCNO 1

F2 - Acquisition Parameters
 Date_ 20170904
 Time_ 12.12 h
 INSTRUM spect
 PROBRD 2108618_0903 ()
 PULPROG zgpg30
 TD 65536
 SOLVENT CDCl3
 NS 1024
 DS 4
 SWH 24038.461 Hz
 FIDRES 0.733596 Hz
 AQ 1.3631488 sec
 RG 199.04
 DM 20.800 usec
 DE 6.50 usec
 TE 295.2 K
 D1 2.0000000 sec
 D11 0.0300000 sec
 TDO
 SFO1 100.6479773 MHz
 NDC1 13C
 P1 10.00 usec
 PLW1 51.7280064 W
 SFO2 400.2316009 MHz
 NDC2 1H
 CPDPRG2 waltz16
 PCPD2 90.00 usec
 PLW2 13.95600033 W
 PLW12 0.33892259 W
 PLW13 0.16966801 W

F2 - Processing parameters
 SI 32768
 SF 100.6379135 MHz
 WDW EM
 SSB 0
 LB 1.00 Hz
 GB 0
 PC 1.40

Figure S19. ¹H NMR and ¹³C NMR spectra of compound 7

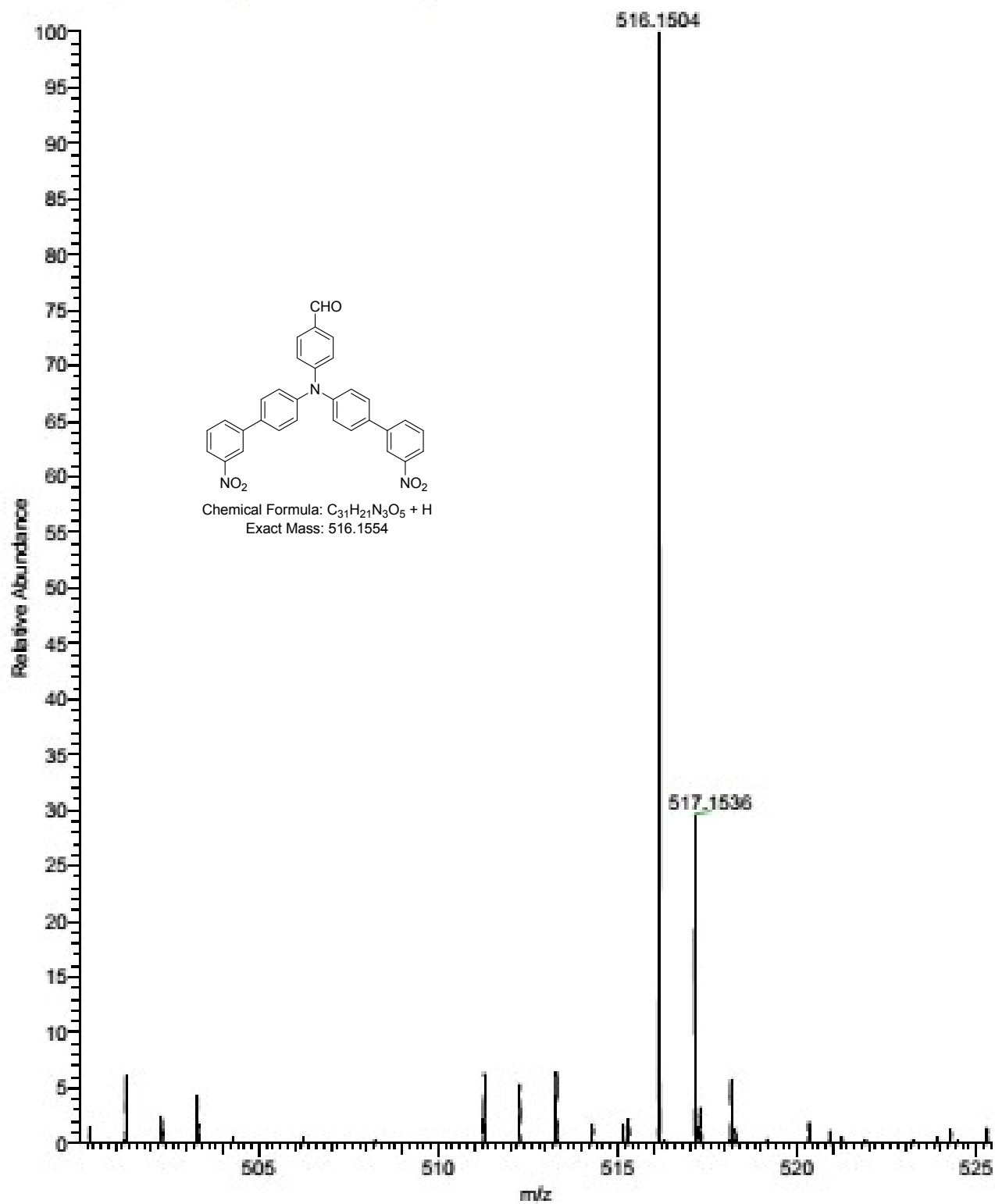


Figure S20. HR-Mass spectra of compound 7

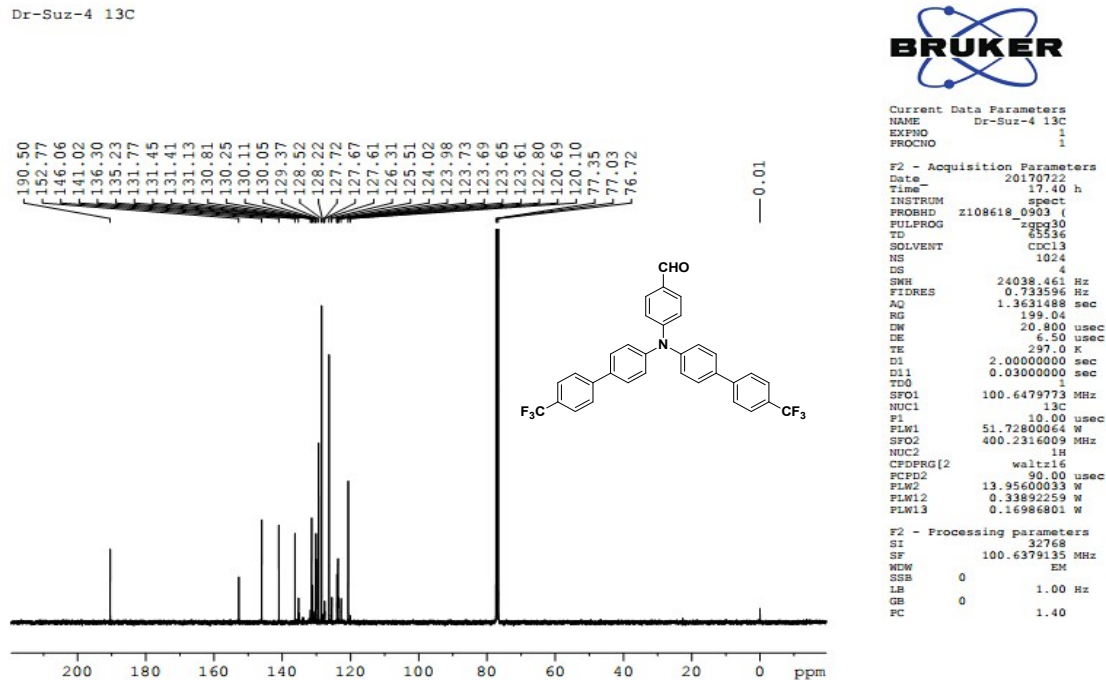
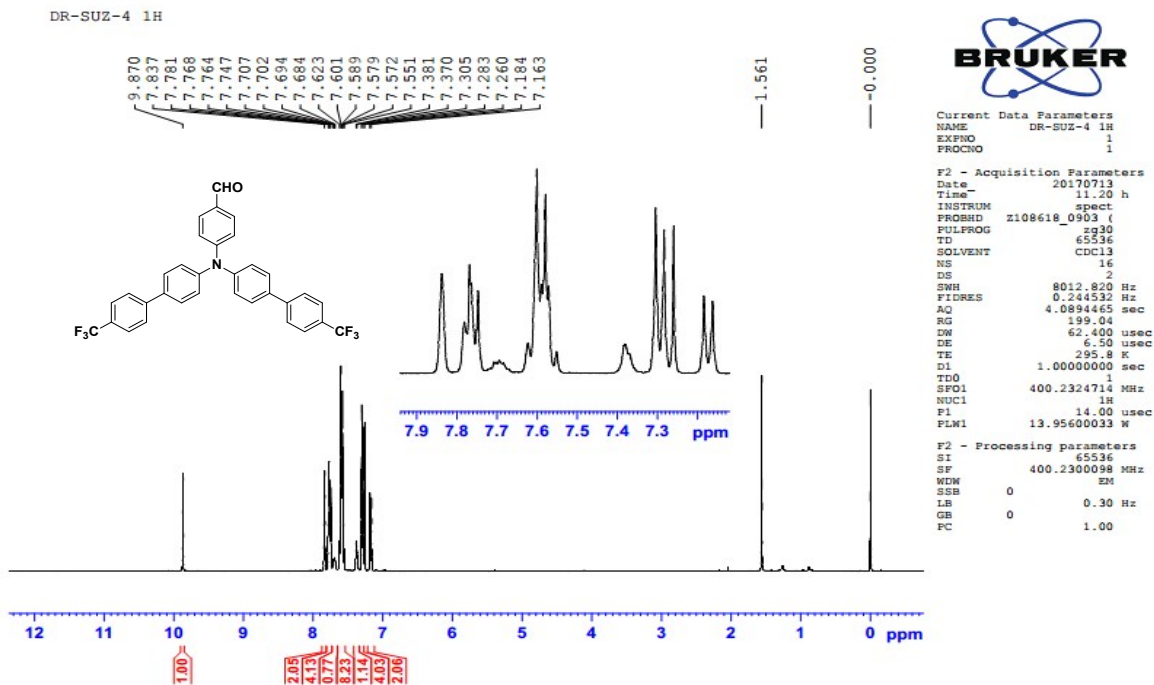


Figure S21. ¹HNMR and ¹³CNMR spectra of compound 8

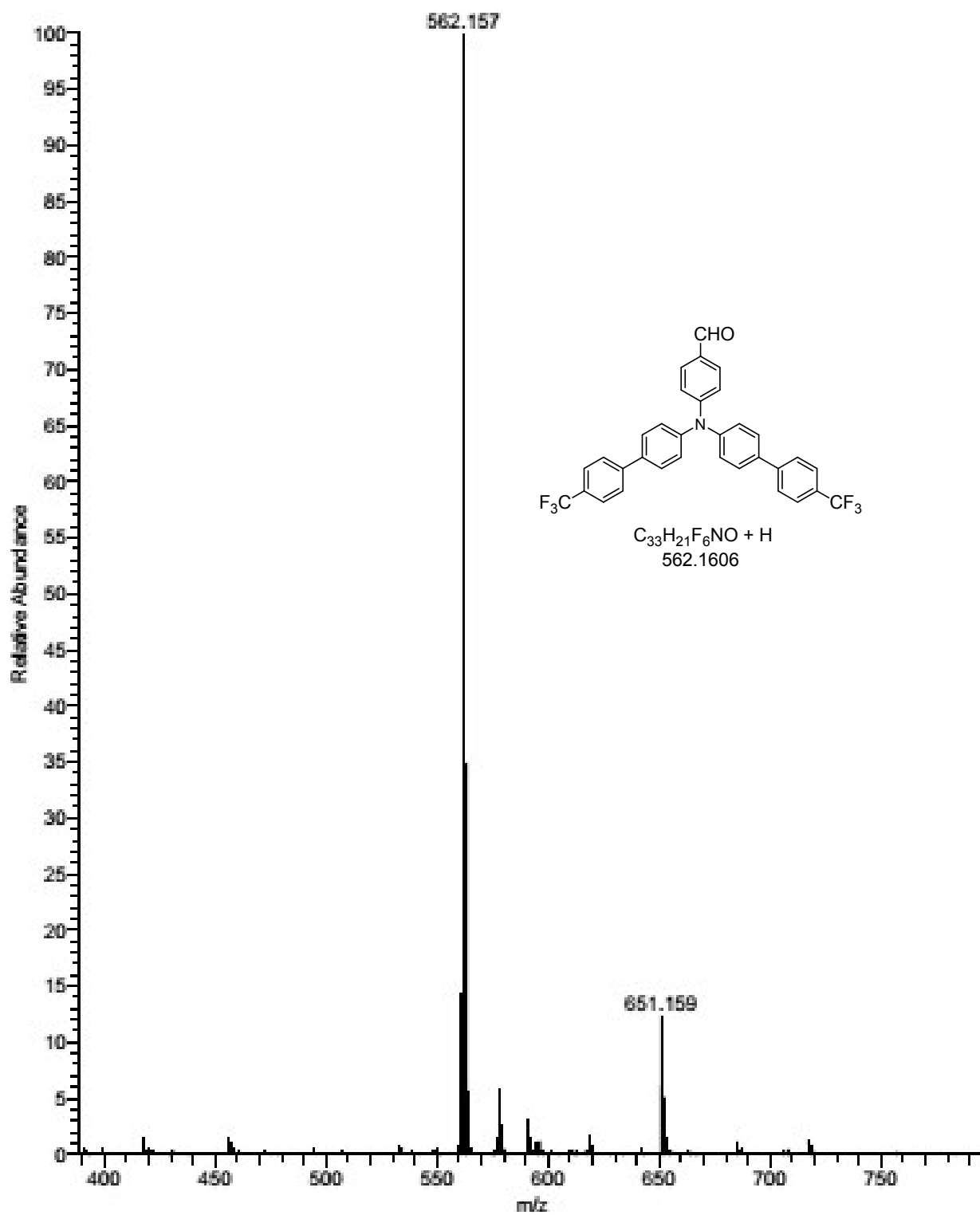


Figure S22. HR-Mass spectra of compound 8

-
- (i) C. Quinton, V. A. Rizzo, C. D. Verdes, F. Miomandre and P. Audebert. *Electrochimica Acta* 2013, **110**, 693.
- (ii) (a) D. Jana and B. K. Ghorai. *Tetrahedron Letters* 2012, **53**, 1798. (b) H. Wang, L.F. Chen. X. Zhu, C. Wang, Y. Wan and Hui Wu. *Spectrochimica Acta Part A: Molecular and Biomolecular Spectroscopy* 2014, **121**, 355.
- (iii) P.P Zamora, K. Bieger, D.Vasquez, M. Merino and R. Maurelia. *Int. J. Electrochem. Sci.* 2015, **10**, 10321.